



저작자표시-비영리-변경금지 2.0 대한민국

이용자는 아래의 조건을 따르는 경우에 한하여 자유롭게

- 이 저작물을 복제, 배포, 전송, 전시, 공연 및 방송할 수 있습니다.

다음과 같은 조건을 따라야 합니다:



저작자표시. 귀하는 원저작자를 표시하여야 합니다.



비영리. 귀하는 이 저작물을 영리 목적으로 이용할 수 없습니다.



변경금지. 귀하는 이 저작물을 개작, 변형 또는 가공할 수 없습니다.

- 귀하는, 이 저작물의 재이용이나 배포의 경우, 이 저작물에 적용된 이용허락조건을 명확하게 나타내어야 합니다.
- 저작권자로부터 별도의 허가를 받으면 이러한 조건들은 적용되지 않습니다.

저작권법에 따른 이용자의 권리는 위의 내용에 의하여 영향을 받지 않습니다.

이것은 [이용허락규약\(Legal Code\)](#)을 이해하기 쉽게 요약한 것입니다.

[Disclaimer](#)

Thesis for the Degree of Master of Engineering

The Influence of Fluoroalkyl Side-Chain
Ratio on Charge Transporting Properties in
DPP-BTZ Copolymer Film: A DFT
Simulation Study with Experimental Support



by

Bright Aryeh Afriyie

Department of Smart Green Technology Engineering

The Graduate School

Pukyong National University

February, 2025

The Influence of Fluoroalkyl Side-Chain
Ratio on Charge Transporting Properties in
DPP-BTZ Copolymer Film: A DFT
Simulation Study with Experimental Support

불소화된 측쇄 비율이 DPP-BTZ 공중합체 박막의
전하 수송 특성에 미치는 영향: 실험 결과가 반영된
DFT 시뮬레이션 연구

Advisor: Professor Jiyoul Lee

by

Bright Aryeh Afriyie

A thesis submitted in partial fulfillment of the requirements for
the degree of

Master of Engineering.

in Department of Smart Green Technology Engineering,
The Graduate School, Pukyong National University

February, 2025

The Influence of Fluoroalkyl Side-Chain Ratio on
Charge Transporting Properties in DPP-BTZ Copolymer
Film: A DFT Simulation Study with Experimental
Support

A dissertation

by

Bright Aryeh Afriyie

Approved by:

Myung-Won Lee, Ph. D. (Chairman)

Jiyoul Lee, Ph. D. (Member)

Kang-Jun Baeg, Ph. D. (Member)

February 21, 2025

Contents

Contents	i
List of Figures	iii
List of Tables	v
Abstract	vi
I . Introduction	1
II . Literature Review	4
1. The Evolution of Organic Semiconducting Materials	4
2. Experimental Study on DPP–BTZ Copolymer	12
3. Computational Study on DPP–BTZ Copolymer	18
4. Theoretical Insight into Charge Transporting Properties of D–A Copolymers	21
III . Methodology	25
IV . Results and Discussion.....	28
A. DPP–BTZ Backbone Curvature	33
B. DPP–BTZ dimer with only Alkyl Side Chains (10:0)	34
C. DPP–BTZ dimer with Alkyl and Fluoroalkyl Side Chains (7:3, 5:5, 3:7)	36
D. Comparing Root Mean Square (RMS) Values	42
E. Stacking Configurations	45
F. DPP–BTZ Backbone Curvature Stacking Configuration	47

G. DPP–BTZ dimer with only Alkyl Side Chains Stacking Configuration (10:0)	48
H. DPP–BTZ dimer with Alkyl and Fluoroalkyl Side Chains Stacking Configuration (7:3, 5:5, 3:7)	50
I. Comparing Root Mean Square (RMS) Values of the Stacking Configurations	55
V. Conclusion.....	57
References.....	58



List of Figures

Figure 1. <i>Trans</i> - and <i>Cis</i> - conformers of polyacetylene	(4)
Figure 2. Organic Electroluminescent device and its materials	(5)
Figure 3. Kekulé structure of a pentacene and a cross section of a pentacene TFT with a plot of $\log_{10}(I_D)$ versus V_{GS}	(6)
Figure 4. (a) Thiophene and (b) P3HT monomeric units with n = number of monomeric units constituting a polymer	(7)
Figure 5. Monomeric units of P3HT and PQT-12 with n = number of monomeric units constituting a polymer	(8)
Figure 6. PBTTC-C14 monomer with n = number of monomeric units constituting a polymer	(8)
Figure 7. Schematic models for "non-liquid-crystalline" polymers and their applicable temperatures: glass transition temperature, T_g , and order-disorder (melting) temperatures, T_m	(10)
Figure 8. Schematic diagrams demonstrating the electronic and ionic charge distribution within a p-n junction structure.....	(11)
Figure 9. Donor and Acceptor units	(12)
Figure 10. Synthetic Approaches of four (4) different kinds of DPP-BTZ.....	(13)
Figure 11. Top-Gate Bottom-Contact type of OFET device architecture	(14)
Figure 12. UV-visible absorption data of solution and film in terms of Alkyl: Fluoroalkyl ratios	(15)
Figure 13. 2D GIXD patterns for the Alkyl: Fluoroalkyl ratios with corresponding 2D GIXD profiles along the In-plane and Out-of plane	(16)
Figure 14. Crystallographic parameter (a) π -distance, (b) coherence length and (c) d -spacing. (d) Twisted polymer backbone according to ratios	(17)
Figure 15. 2D models of (a) Th-DPP-Th-BTZ-Th monomer, (b) Fu-DPP-Fu-BTZ-Fu monomer and their polymeric units.....	(18)
Figure 16. Simulation Box	(19)

Figure 17. (a) Optimized geometries of isolated molecules in vacuum (B3LYP/6-31G(d)) with values of the backbone curvature angle Ω , (b) parallel, and (c) anti-parallel stacks (20)

Figure 18. Charge Carrier Hopping in a localized system (22)

Figure 19. PES for D-A complex in a harmonic approximation (23)



List of Tables

Table 1. Differences between n-type, p-type and ambipolar charge transport. (11)



불소화된 측쇄 비율이 DPP-BTZ 공중합체 박막의 전하 수송 특성에 미치는 영향: 실험 결과가 반영된 DFT 시뮬레이션 연구

Bright Aryeh Afriyie

스마트그린기술융합공학과

국립부경대학교

Abstract

Diketopyrrolopyrrole (DPP) 기반 도너-수용체 (D-A) 형 공중합체는 높은 전계효과 이동도와 함께 p형 및 n형 전하를 모두 전달할 수 있는 양극성 특성으로 인해 유기반도체 전자소자 연구자들로부터 많은 주목을 받고 있다. 본 연구에서는 유기전계효과 트랜지스터 (Organic Field-Effect Transistors, OFETs)의 채널로 사용된 Diketopyrrolopyrrole-Benzotriazole (DPP-BTZ) 기반 반도체성 공중합체의 알킬 대 불소화알킬 측쇄 비율을 10:0, 7:3, 5:5, 3:7로 조정했을 때, 관찰된 OFET 성능 변화의 원인을 밀도 범함수 이론 (DFT) 시뮬레이션을 통해 검증하였다. 특히, DPP-BTZ 반도체성 공중합체의 알킬 대 불소화알킬 측쇄 비율이 고분자 골격의 평면성에 미치는 영향을 뒤틀림 각도와 에너지 측면에서 분석하였으며, 그 결과 DPP-BTZ 공중합체의 적층 구조가 3.5 Å의 π - π 적층 거리에서 골격 평면성을 결정하는 중요한 요소임을 확인하였다. 결론적으로, 본 연구에서는 밀도 범함수 이론 시뮬레이션을 통해 측쇄 설계가 골격 평면성 및 효율적인 전하 이동을 가능하게 하는 고성능 D-A형 반도체 공중합체 설계에 필수적임을 입증하였다.

I . Introduction

Organic Field-Effect Transistors (OFETs) have advanced from lust of learning to interestingly-adventurous field of study in the last couple of decades. This keen interest in OFETs emanates from the relatively inexpensive thermal budget required to fabricate these devices, the ability of organic materials to act as good insulations and also their high degree of mechanical flexibility which make them very useful in flexible displays, mechanical sensors and radio frequency identification tags.

The discovery of D-A structural analog of a silicon p-n junction imprinted the emergence of an intensive research into characterizing and fabricating of these OFETs. Donor - Acceptor type semiconducting copolymers have alternating electron-donating unit (D) and electron-accepting units (A) along the polymeric backbone but these emerging materials such DPP-BTZ copolymer exhibits amorphous-like structural characteristics which is similar to classical semiconducting polymers but have more efficiency in terms of different charge transporting mechanism. This is the driving force for the experimental study. Though these D-A based semiconducting materials have keen interest in recent times, there are a number of unanswered questions as to the role of order-disorder interplay in their charge mobilities, how their crystalline structure, whether partially or not, involved in their charge transporting mechanisms, and also how the planarity of their backbone curvature, whether influenced by side chains or not, facilitate or impedes charge transporting properties.

Diketopyrrolopyrrole–Benzotriazole, DPP–BTZ is considered as an ambipolar type because it possesses both the p–type which is the DPP (electron–donor) and the n–type which is the BTZ (electron–acceptor) in facilitating a “self” charge transport. DPP–based semiconducting materials are recognized as the highest performing ambipolar D–A polymers with FET mobilities up to $12 \text{ cm}^2\text{V}^{-1}\text{s}^{-1}$ for hole–transport and up to $6.3 \text{ cm}^2\text{V}^{-1}\text{s}^{-1}$ for the electron–transport.

In the experimental study, we developed a device architecture which involves a copolymerization of a synthesized dithienyl –DPP– based polymer with benzotriazole (BTZ) monomer. Their TFTs were fabricated and characterized with the outmost research goal of elucidating the effect on charge transport after fluorine doping using the sidechain engineering technique. Four types of DPP–BTZ copolymers, in the ratios of alkyl to fluoroalkyl sidechain of 3:7, 5:5, 7:3, and 10:0, were synthesized. Contrary to our research expectation, the electron and hole mobilities decreased though there was an introduction of an electrophilic atom such as fluorine. Results from UV– visible spectroscopy and 2D Grazing Incidence depicts that the torsional angle of the polymer main chain has a greater influence on charge transport within the DPP–BTZ semiconductor compared to the intermolecular gap. These experimental findings triggered a comprehensive insight into the mechanistic activities at a computational level of theory.

The interest in the DFT simulation study of the DPP–BTZ copolymer focuses on the geometrical orientation of the DPP–BTZ copolymer in terms of torsional angles of the copolymer undergoes charge transporting mechanism. In order to affirm the fact that “the more planar and rigid the backbone curvature of an organic

semiconducting materials is, the more efficient the charge transport hence the higher the performance of the OFETs”, this study seeks to use the torsional angles of the backbone curvature to determine the planarity and rigidity of the DPP–BTZ copolymer.

Also, this DFT simulation study seeks to validate, interpret and/or predict an experimentally observed trend during the side chain engineering in terms of alkyl: fluoroalkyl sidechains ratios of 10:0, 7:3, 5:5 and 3:7.



II. Literature Review

1. The Evolution of Organic Semiconducting Material

Organic Semiconducting materials can be traced back to the 1950s and 1960s, where their maiden discoveries centered around organic dyes and charge transfer complexes. The most predominant material used, anthracene, which is an organic crystal, was primarily for photoreceptors in photocopying and organic light-emitting devices.

In 1970s, *Shirakawa et al* were working on polymerization of acetylene into plastics by using a hyper-catalytic amount of a Ziegler-Natta catalyst. Out of serendipity, they invented an insulating π -conjugated polyacetylene, that act like a conductor with conductivity of 10^3 S/cm, by iodine doping. Their accidental discovery, which awarded the Nobel prize in 2000, made scientists regarded polyacetylene as an excellent polymeric material to be a “synthetic metal” because of its conjugated double bonds.

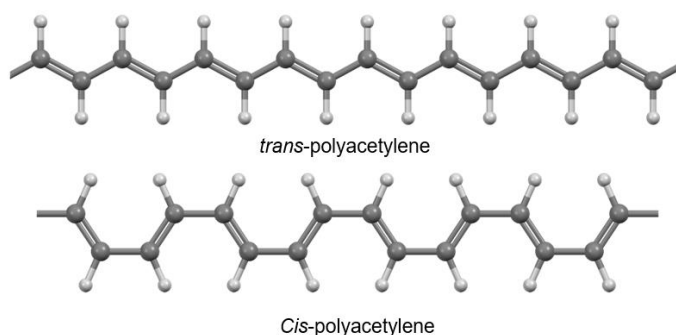


Figure 1. *Trans*- and *Cis*- conformers of polyacetylene.

The electrically conductive in these polymeric materials revolve around the principle of doping: where there are freely moving electrons in the polymers, which are not bounded by the atoms, thus in a process postulate that there is an electron withdrawal through oxidation to form a hole or addition of electron through reduction.

In 1980s, *Chen et al* had a breakthrough in Organic electroluminescent devices (OLEDs). They investigated the impact of doping blue-emitters Alq (BA1q) molecules with blue-emitting (perylene) and red-emitting (DCJTM) fluorescent molecules to emitting colors form blue to orange which included white. There were several alterations done by substitution at the 2 and 4 positions of BA1q produced a significant blue shift in the emission peak comparative to the green Alq which enhanced the fluorescence quantum efficiency. Their doping did not only shift the emission spectrum along with improving the operational stability of the devices (OLEDs) which optimized the performance and durability of the devices.

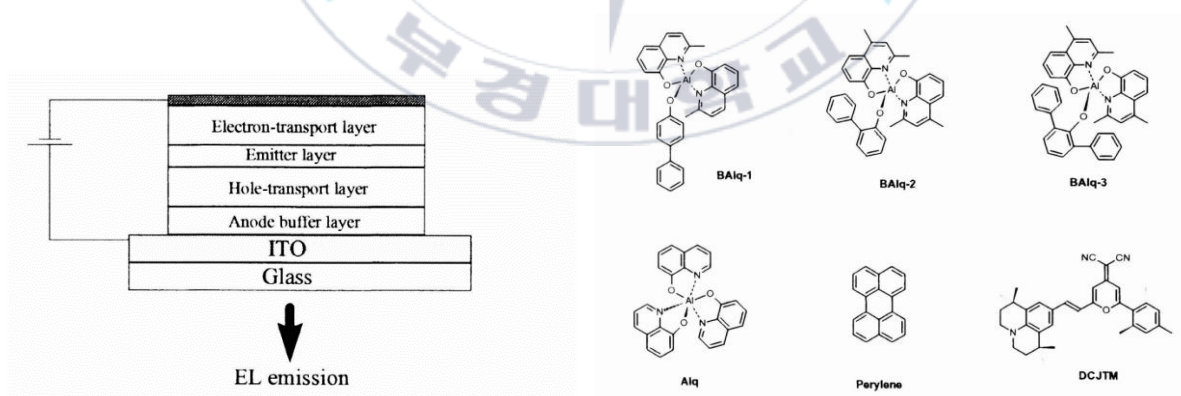


Figure 2. Organic Electroluminescent device and its materials.

In 1990s, *Klauk et al* were attributed to the breakthrough of Organic Field-Effect Transistors (OFETs). They delved into developing organic thin film transistors (TFTs) using fused-ring polycyclic aromatic hydrocarbon pentacene as the active electronic material where they achieved field-effect mobility larger as $0.7\text{cm}^2/\text{V}\cdot\text{s}$ and an on/off current ratio higher than 10^8 . Both values were compared to hydrogenated amorphous silicon device and it was elucidated that even though the organic TFTs have undesirably large subthreshold slope, it was not the intrinsic property of organic semiconducting materials thus there are possible similarities.

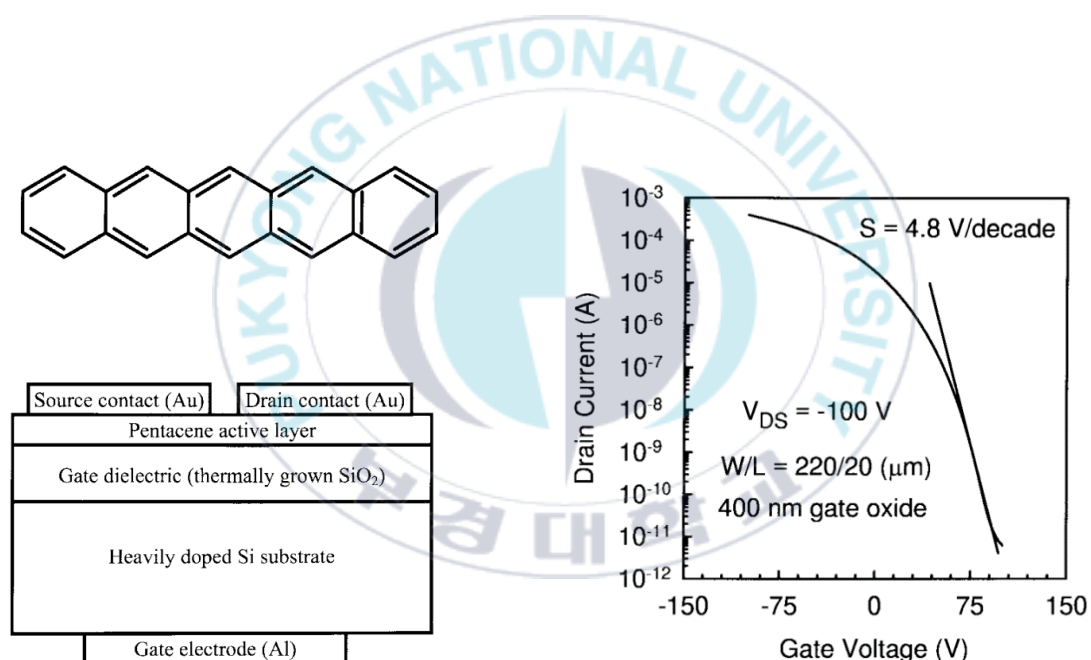


Figure 3. Kekulé structure of a pentacene and a cross section of a pentacene TFT with a plot of $\log_{10}(I_D)$ versus V_{GS} .

The evolution of organic semiconducting materials developed from small molecules to polymers. Comparatively to silicon, Polythiophene was commonly used because it was cheap, structurally flexible, processability at low temperature, and more

importantly the high charge transport characteristics. There were so many tests on P3HT, which was the most popular polythiophene used, and the results depicted that:

(a) The coupling of head-tail (HT) in the P3HT Regio-regular arrangement yielded larger mobilities as compared to Regio-random arrangement (TT and HH) among the three types of couplings: head-head (HH), tail-tail (TT), and head-tail (HT) couplings.

(b) This Regio-arrangement could obtain two types of adjustments on the substrate: Face-on direction or Edge-on direction.

(c) The mobilities of the Edge-on direction fell within $0.05 - 0.2 \text{ cm}^2\text{V}^{-1}\text{s}^{-1}$ which gave noticeably two orders of magnitude greater than the Face-on direction.

There was a practical limitation as to the usefulness of P3HTs which was due to their greater HOMO energy states. In an attempt to enhance the usefulness of OFETs, their first attempt was to introduce a Regio-regular alkyl chain unto the pi-conjugated backbone of the polymer-thiophene (A) which ameliorated the solubility of the polymer (because of the alkyl groups) but analogously rise the HOMO energy states of the polythiophenes. This made the P3HT polymer (B) high unstable to air.

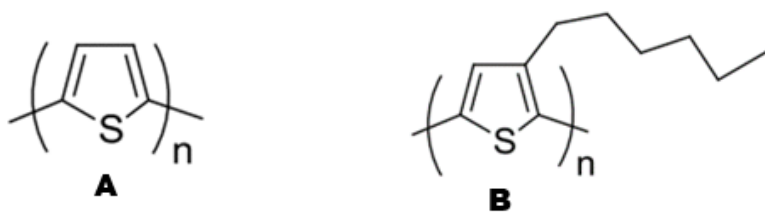


Figure 4. (a) Thiophene and (b) P3HT monomeric units with n = number of monomeric units constituting a polymer.

Ong et al did a series of polythiophenes research with alkyl chains substituted on only half of the thiophene rings. Comparatively to polymer B, their mobilities unveiled

large mobilities of $0.14 \text{ cm}^2\text{V}^{-1}\text{s}^{-1}$ and had a lower HOMO energy state with good stability.

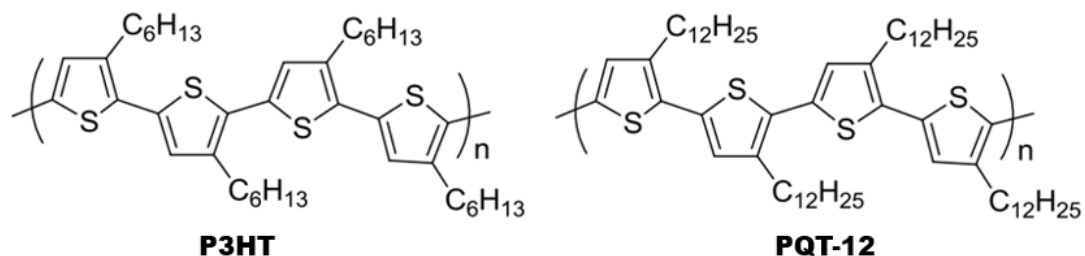


Figure 5. Monomeric units of P3HT and PQT-12 with n = number of monomeric units constituting a polymer

McCulloch et al synthesized polymers containing thieno [3,2-*b*] thiophene and he observed that the resonance energy of the condensed phase of the thiophene ring was greater than the single thiophene ring therefore, the electron delocalization is less probable from the fused thiophene ring into the backbone curvature. The HOMO energy state of the polymer was lowered by the Electron delocalization reduction. The carrier mobilities of PBTTT C-14 lies between $0.2 - 0.6 \text{ cm}^2\text{V}^{-1}\text{s}^{-1}$ (which is large) and when evaluated on annealed equipment in a presence of N_2 gas, carrier mobility of PBTTT C-14 moves as high as $0.7 \text{ cm}^2\text{V}^{-1}\text{s}^{-1}$ using $5 \mu\text{m}$ channel length devices.

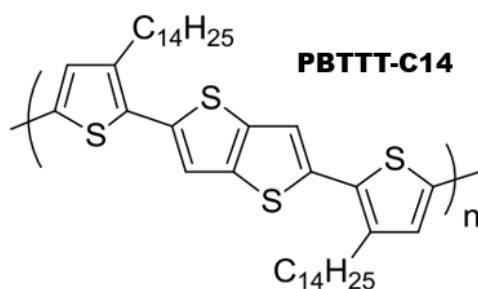


Figure 6. PBTTT-C14 monomer with n = number of monomeric units constituting a polymer.

According to *Marina et al*, these semiconducting polymers are categorized into amorphous state and semi-crystalline state. For the amorphous state, the semiconducting materials are characterized because they lack a long-range order hence adopting some disordered coil-like conformations due to the large number of possible rotational isomeric states of their polymeric chains. They also exhibit a glass transition temperature (T_g) yet do not have a distinct melting temperature (T_m) since they do not form crystalline structures.

Unlike the amorphous state, the semi-crystalline materials are polymeric chains that are highly orderly arranged. These materials exhibit both glass-transition temperature (T_g) and a melting temperature (T_m) since they consist of both crystalline and amorphous. The crystalline regions have an impact on their higher mechanical strength and stability whereas the amorphous regions make them flexible.

For the Semi-paracrystalline state, it bridges the gap between the amorphous state and the semi-crystalline state by the presence of small paracrystalline domains embedded in a more distorted matrix. Uncharacteristic of semi-crystalline materials, these paracrystalline domains are highly distorted and do not exhibit long-range order in a semi-crystalline material.

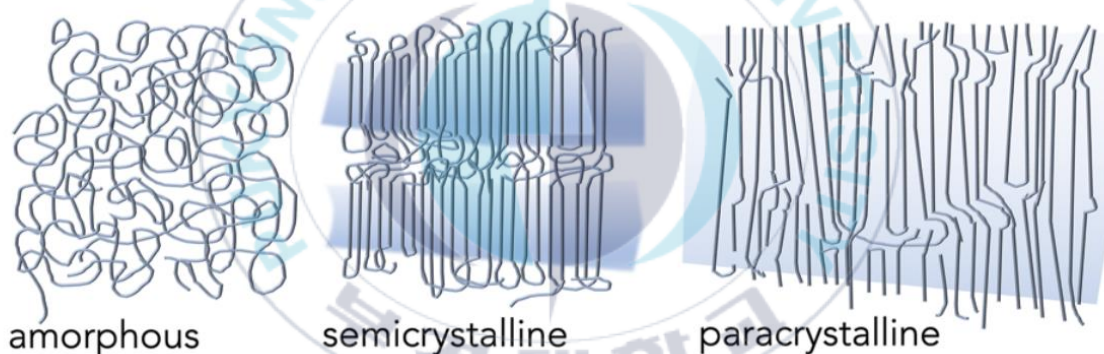
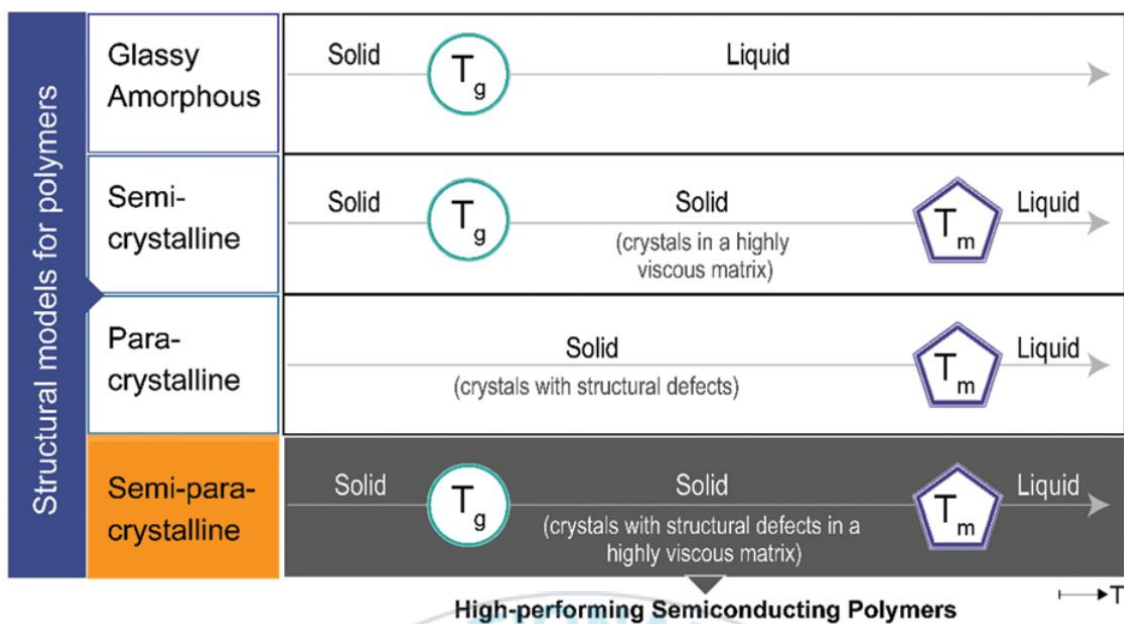


Figure 7. Schematic models for “non-liquid-crystalline” polymers and their applicable temperatures: glass transition temperature, T_g , and order-disorder (melting) temperatures, T_m .

Charge mobility is a pivotal yardstick for the high performance of semiconducting materials and have chosen a cross section of systems focusing on p-type materials with mobilities in excess of $1 \text{ cm}^2/\text{Vs}$ and n-type materials with mobilities above $0.1 \text{ cm}^2/\text{Vs}$. The charge transport in semiconducting materials occurs when the movement of charge carriers such as electrons (negatively charged), holes

(positively charged) or both in a semiconducting material. The table below briefly outlines the difference between n-type, p-type and ambipolar charge transport.

Charge Transport	N-type	P-type	Ambipolar
Majority Carriers	Electrons	Holes	Electrons and Holes
Dopants	Electron donors	Electron acceptors	Dependent on semiconducting material
Conduction Mechanism	Conduction band	Valence band	Both

Table 1. Differences between n-type, p-type and ambipolar charge transport.

To enhance charge mobility, *Matyba et al* did some semiconducting device architecture whereby stacking two different types of semi-conductor: a p-type containing excess holes and an n-type with excess electrons which causes an intrinsic electric field at the surface called the p-n junction.

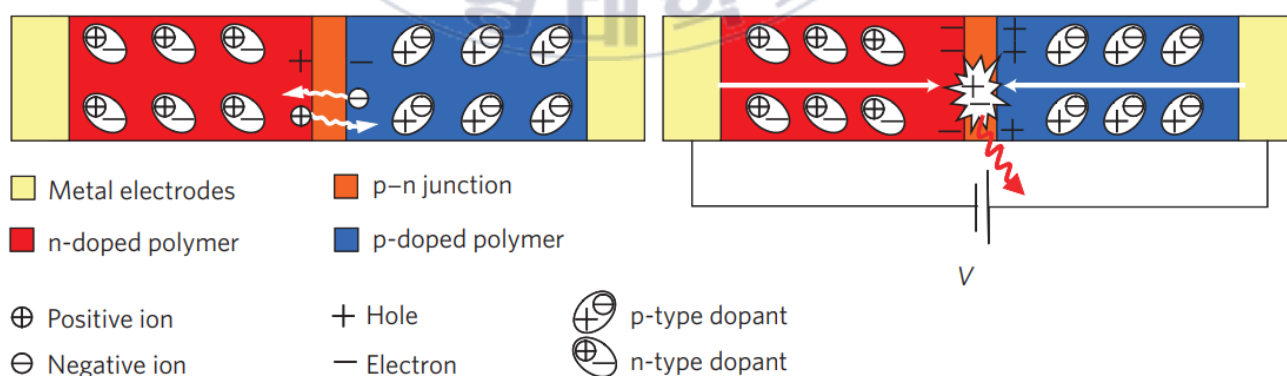


Figure 8. Schematic diagrams demonstrating the electronic and ionic charge distribution within a p-n junction structure.

Undoubtedly, the donor–acceptor (D–A) strategy, popularly called the ambipolar type, was developed by *Havinga et al.* This design motif of D–A conjugated polymer enhances partial charge transfer between the electron donor and the acceptor moieties hence decreasing the bond length alternation in the repeating unit then finally, reduce the band gap. They are sometimes called the “push–pull” conjugated polymers. The stronger the electron–donating and electron–accepting tendencies of the donor and acceptor unit respectively, the more important in determining the energy levels and the bandgap of the D–A copolymer. A stronger donating unit increases the HOMO orbital level whereas a stronger acceptor unit decreases the LUMO orbital level, narrowing the band gap of the D–A polymer.

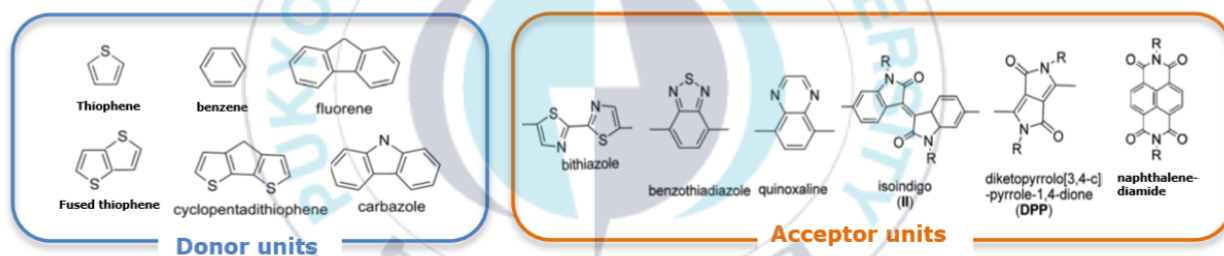


Figure 9. Donor and Acceptor units.

2. Experimental Study on DPP–BTZ Copolymer

DPP–BTZ Copolymer categorized as a donor–acceptor conjugated copolymer because the diketopyrrolopyrrole (DPP) and Benzotriazole (BTZ) exhibiting electron donor and electron acceptor respectively.

Nielsen et al did comprehensive research on DPP–based polymers using a field–effect transistors. They did a comparison for more than 80 different DPP containing polymers, discussing their synthesis, their molecular structures, their correlation

between structures and electronic properties, and their charge mobilities. They elucidated the side chains attached to the DPP-core were endowed with solution processibility. They also brought to bear that side chain substitution exerted an integral role on the influence of the packing and backbone conformation of conjugated polymers.

Gruber *et al* synthesized four DPP-BTZ copolymers which are (I-C18)-DPP-(b-C17)-BTZ, (I-C18)-DPP-(I-C8)-BTZ, (b-C20)-DPP-(I-C8)-BTZ and (I-C16)-DPP-(I-C8)-BTZ. The first two (2) DPP-BTZ were synthesized by Suzuki polycondensation method and the remaining two (2) DPP-BTZ were prepared by Direct arylation polymerization method in order to synthesize DPP-BTZ copolymers.

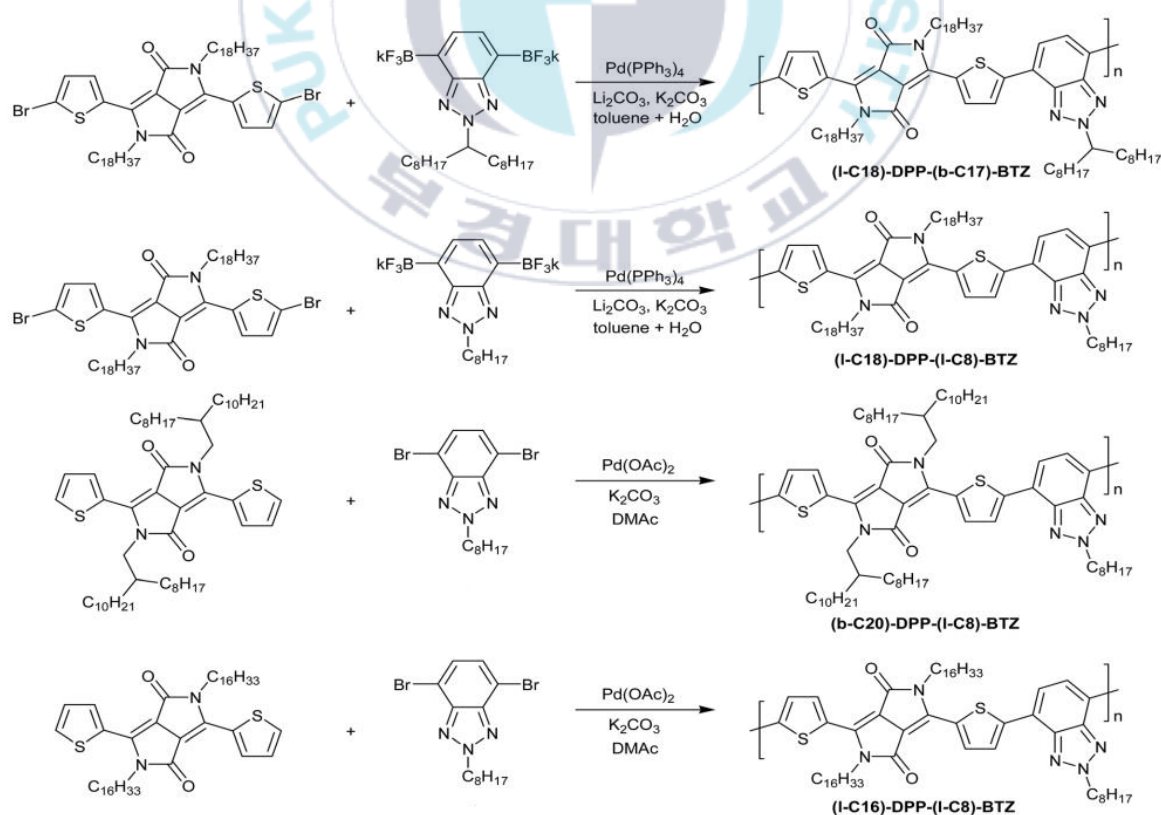


Figure 10. Synthetic Approaches of four (4) different kinds of DPP-BTZ.

Though *Gruber et al* synthesized four different kinds of DPP–BTZ, our experimental research used the (I–C18)–DPP–(b–C17)–BTZ copolymer based on the clear semicrystalline and with different texture at h00 peaks along the Q_{xy} , it exhibited a highly ordered crystalline structure. It also had an improved solubility even as it had the highest number of sidechains which did not affect the π – π stacking, and most importantly it showed the highest FET performance with high I_{on}/I_{off} ratios of 10^6 to 10^7 at low source–drain voltages, $V_D = -5$ V, low subthreshold swing values of 1.5 V dec $^{-1}$ and high average saturated hole mobilities of 2.4 cm 2 V $^{-1}$ s $^{-1}$ with maximum values for hole mobilities ranging up to 2.8 cm 2 V $^{-1}$ s $^{-1}$.

We used the Top–Gate, Bottom–Contact type of OFET device architecture because the Top–Gate structure has an external gate structure that makes it less exposed to the semiconductor layer and also the Bottom–Contact structure has a high contact resistance.

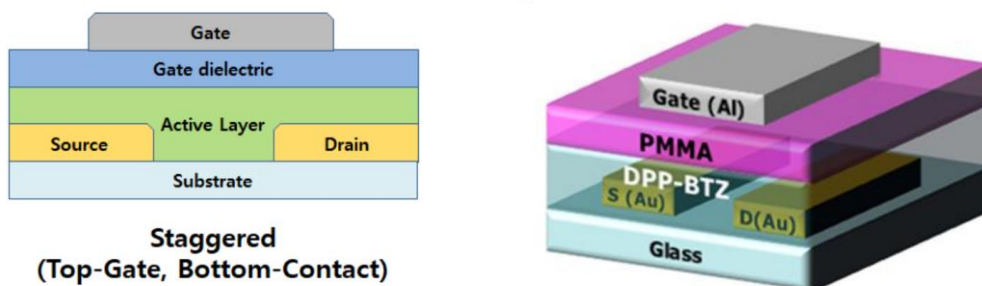


Figure 11. Top–Gate Bottom–Contact type of OFET device architecture.

The alkyl to fluoroalkyl side chains were fabricated in the ratio of 10:0, 7:3, 5:5 and 3:7 where the DPP–BTZ was the polymeric backbone. The UV–visible absorption data of solution and film was measured to elucidate the band gap energies. The band gap energies for the four alkyl– to–fluoroalkyl ratios were all at 1.32 eV.

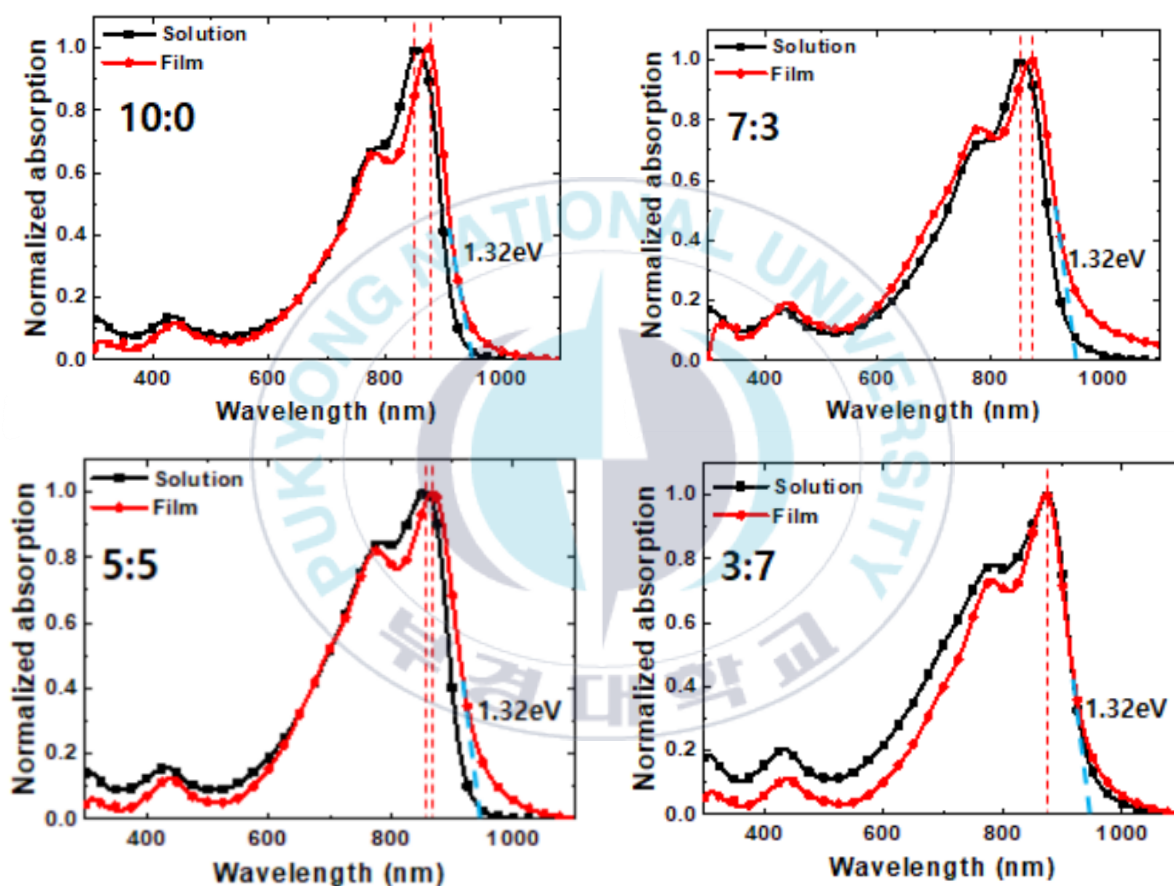


Figure 12. UV–visible absorption data of solution and film in terms of Alkyl–to–Fluoroalkyl ratios.

From this data, it was elucidated the molecule orientation had a significant influence on the charge transport. The interactive mode of “cylindrical” molecules had an influence on the molecular aggregation type: where the “side–by–side” orientation is the H–aggregates and the “head–to–tail” pair orientation is the J–aggregates. As the ratio of the fluoroalkyl side chain increases, the absorption peak wavelength

demonstrated a shift from red-shifted absorption spectra to blue-shift which depicted a decrease in the planarity of the DPP-BTZ backbone curvature.

The degree of crystallinity based on the four ratios were analyzed using 2D Grazing Incidence X-ray Diffraction (2D GIXD). The Face-on and Edge-on crystals coexist after observing the $h00$ and $0h0$ peaks. As the ratio of fluoroalkyl side chain increased, the face-on crystal shifted to an edge-on crystal.

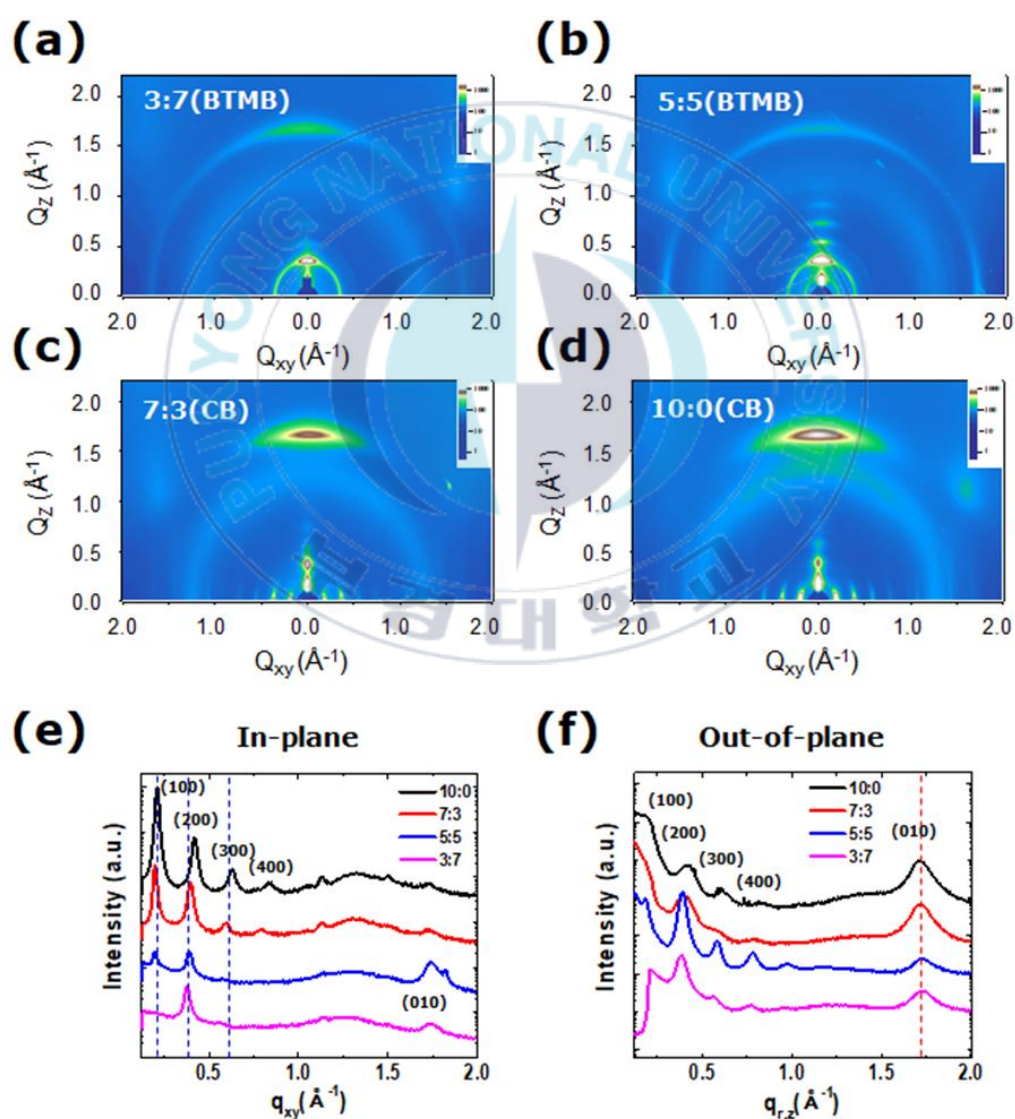


Figure 13. 2D GIXD patterns for the Alkyl: Fluoroalkyl ratios with corresponding 2D GIXD profiles along the In-plane and Out-of plane.

Also, according to the 2D GIXD crystallographic graph, the π - π stacking distance becomes shorter as the fluoroalkyl side chain ratio increases which improves charge transport. Nevertheless, as π - π stacking distance increases, there is a sufficient overlap between the π -orbitals, there is no much significant change in the charge transport. As the ratio of fluoroalkyl sidechain decreases, the π -distance increases, yet we assumed the torsional angle of the DPP-BTZ backbone curvature decreases because of the electrophilic nature of the fluorine.

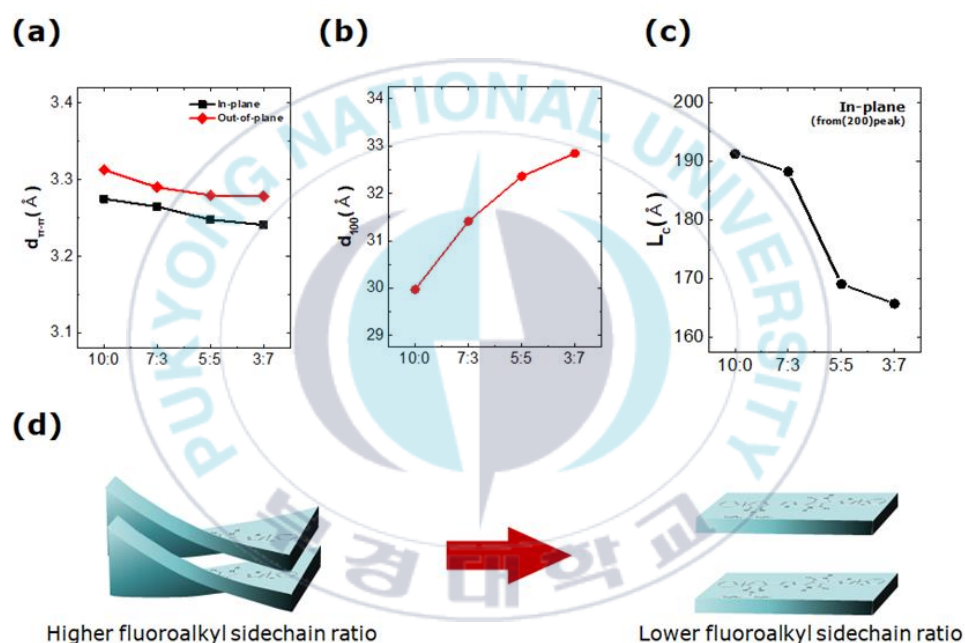


Figure 14. Crystallographic parameter (a) π -distance, (b) coherence length and (c) d-spacing. (d) Twisted polymer backbone according to ratios.

We observed trends in the ratio of alkyl to fluoroalkyl chains were manipulated which triggered a computational insight into the influence of fluoroalkyl on the charge transporting properties of the DPP-BTZ copolymer.

3. Computational Study on DPP–BTZ

To the best of our knowledge, there is no precise study on Density Functional Theory (DFT) simulation on the Charge Transporting Properties along backbone curvature of the DPP–BTZ copolymer.

The closest study is where they proved that the design of the DPP–BTZ copolymers could effectively modulate their charge transporting properties by accurately selecting the linkers and side chains.

In their study, they linked together the DPP and BTZ with furan or thiophene then considered their morphology, electronic, and intrinsic transport properties at angstrom resolution in computational simulation with experimental support. They modeled four monomeric units containing two different linkers connecting electron-withdrawing core units with two alkyl substituents (linear dodecyl and branched 2-octyldecyl side chains) at lactam nitrogen of the DPP core.

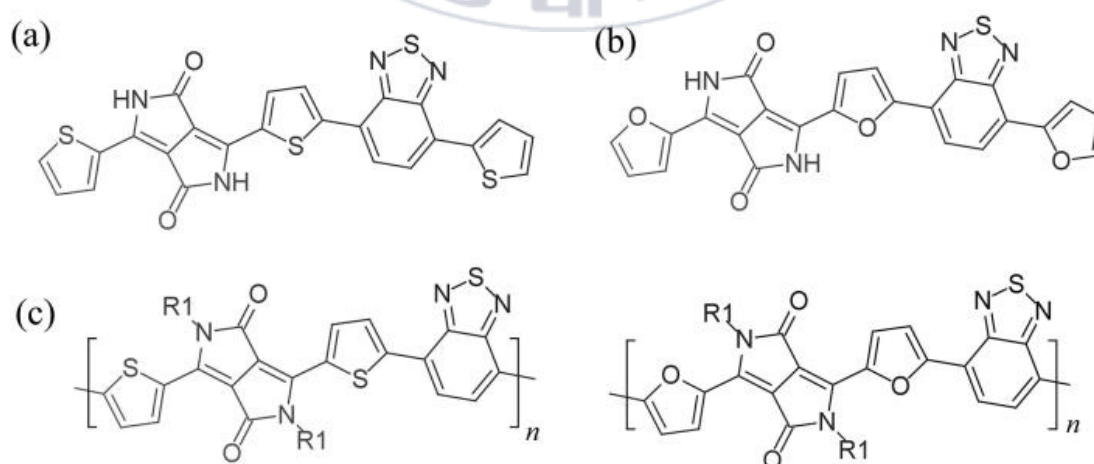


Figure 15. 2D models of (a) Th–DPP–Th–BTZ–Th monomer, (b) Fu–DPP–Fu–BTZ–Fu monomer and their polymeric units

They found out that the monomers of the copolymers had very similar electronic and optical properties yet the difference between them as their linker (whether furan or thiophene). Also, the furan-containing monomers were more curved whereas the thiophene-linked monomers were more stretched. The branched side chains affected the planarity of the macromolecules, which led to a longer π - π stacking and lamellar distances in the simulation box.

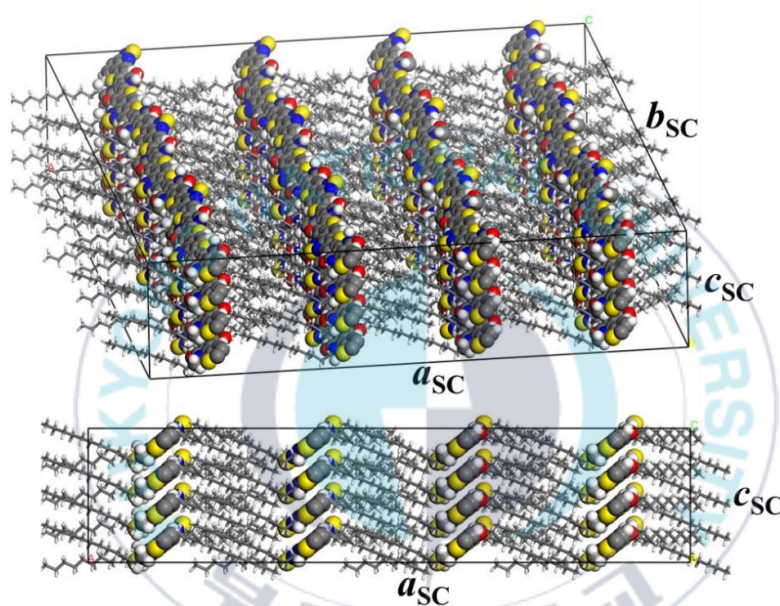


Figure 16. Simulation Box.

The curvature angle (Ω) was measured at 57.8° for the furan-linked backbone and 45.1° for the thiophene-linked backbone, making the furan-linked more curved and the thiophene-linked chain more stretched. The more curved furan-linked of the backbone curvature, the higher electron mobilities in certain stacking configurations leading to unbalanced ambipolar transport properties.

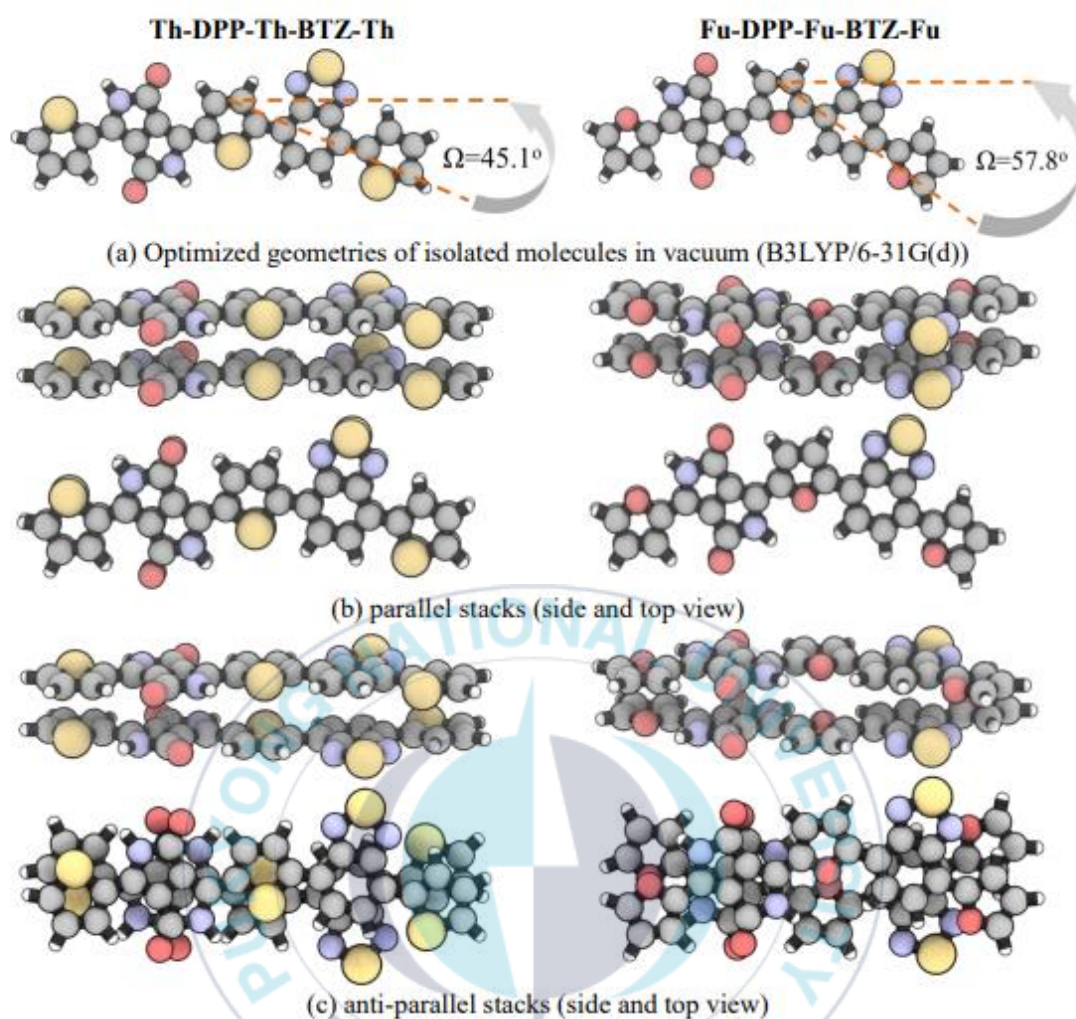


Figure 17. (a) Optimized geometries of isolated molecules in vacuum (B3LYP/6-31G(d)) with values of the backbone curvature angle Ω , (b) parallel, and (c) anti-parallel stacks.

For their molecular dynamics study, their research objectives were what happens to the stacking upon thermal annealing, are similar acceptor blocks and donor linkers segregated, mixed, or disordered in the DPP-BTZ conjugated stacks and lastly the influence of heteroatom in the linker and the branching of the substituents on the DPP?

4. Theoretical Insight into Charge Transporting Properties of D–A Copolymers

Charge transport mechanisms together with their descriptions can be dependent on the degree of the structural order in organic semiconducting materials. The band transport is observed at extreme circumstances of highly purified molecular crystals at low temperatures. This observation depicts that charge carriers are delocalized and their mobilities are determined from their effective masses and the mean relaxation time of the band states. The weakness of the electronic delocalization in organic semiconductor has similarity to an inorganic semiconductor (typically only a few $k_B T$ at room temperature). Hence, the mobilities at room temperature in molecular crystals, range from 1 to 10 cm²/Vs only. The power law temperature dependence of charge mobility is a characteristic feature of band transport:

$$\mu \propto T^{-n} \text{ with } n = 1 \dots 3$$

and mobility decreases with increasing temperature.

Another extreme case is for amorphous solids, where the charge carriers are strongly localized. In this case, charge transport can be reported by the charge carriers hopping between localized states in entire molecules or conjugated segments for polymers.

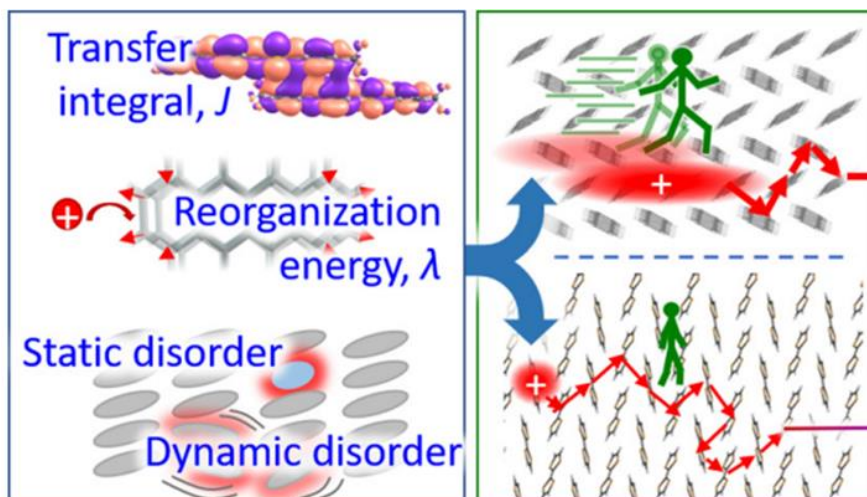


Figure 18. Charge Carrier Hopping in a localized system

For the temperature-dependent hopping process, it showed an activated behavior and also an applied electric field, E :

$$\mu(E, T) \propto \exp [(-\alpha/k_B T)^2] \cdot \exp (\beta \sqrt{E})$$

where α and β are numerical constants, $k_B T$ is called the thermal energy

For organic semiconductors, the intermolecular interactions are weak which means the donor $|D\rangle$ and acceptor $\langle A|$ units can be approximated by the non-interacting molecular orbitals, or diabatic states, and the electronic Hamiltonian takes its *tight-binding* form:

$$H^{\text{el}} = E_D |D\rangle \langle D| + E_A |A\rangle \langle A| + J (|D\rangle \langle A| + |A\rangle \langle D|)$$

where E_D , E_A are the individual site energies, J is called the electronic coupling (transfer integral) for the two states.

To describe the charge transfer reactions, the nuclear motion needed to be considered. Hence, the reaction coordinate (q) which relates to the actual position

of the nuclei that connects the donor and acceptor states. To simplify the derivation, all the nuclear motions were treated classically, hence the Potential Energy Surface (PES) for the initial and final states became harmonic with identical curvatures even though there can be different curvatures for the initial and the final states.

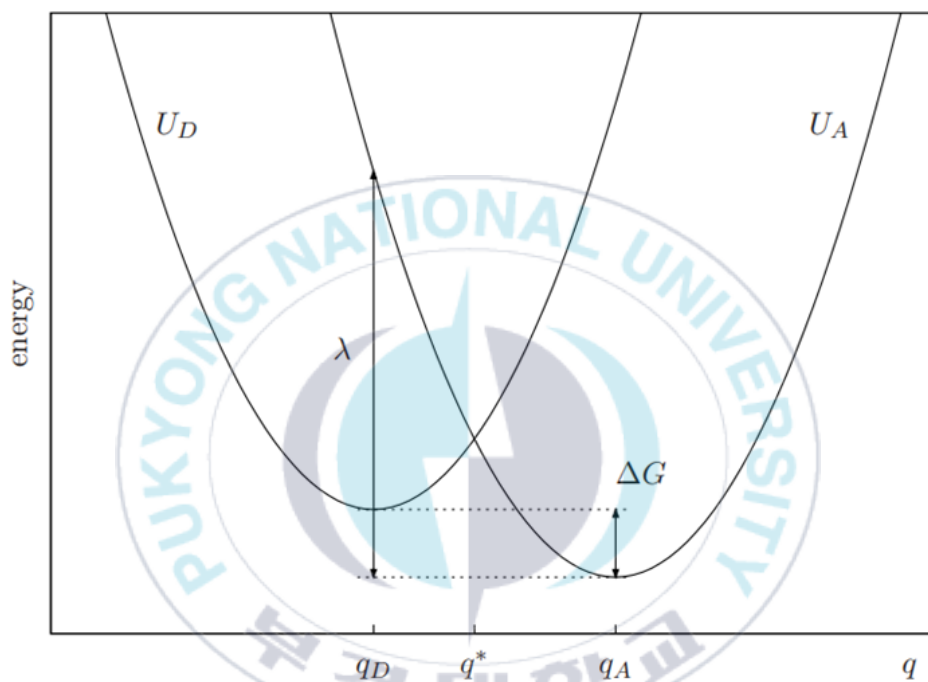


Figure 19. PES for D–A complex in a harmonic approximation

For the parabolic PES approximation, the integration can be carried out analytically that is; the number of vibrational degrees of freedom becomes macroscopic in a high-temperature limit giving an equation called Marcus Charge Hopping rate.

$$k_{DA} = \frac{2\pi}{\hbar} |J|^2 \sqrt{\frac{1}{4\pi k_B T \lambda}} \exp[-(\Delta G + \lambda)^2 / 4\lambda k_B T]$$

where λ is the Reorganization energy, ΔG is the reaction driving force (differences between the PES minima)

Reorganization energy is one of the crucial determinants for the rates of Charge

transport. It is divided into two parts:

- Inner contributions emanate from the charges at equilibrium geometry of D–A units in charge transfer reaction.
- Outer contributions also emanate from the electronic and nuclear polarization/relaxation of the surrounding medium.



III. Methodology

It is very important to come to terms with the aim of performing an electronic structure calculation is to predict charge transporting characteristics that can be compared with the experimental results. The question then comes “How accurate are the Density Functional Theory (DFT) calculations?”. It is very necessary to recognize that despite the apparent simplicity of this question, it is not well posed. The notion of accuracy includes multiple ideas that need to be considered separately. In particular, it is useful to distinguish between physical accuracy and numerical accuracy.

For physical accuracy, the aim is to understand how precise the predictions of a DFT calculation for a specific physical property are relative to the true value of that property as it would be measured in a perfect (often hypothetical) experimental measurement. In contrast, numerical accuracy assesses whether a calculation provides a well-converged numerical solution to the mathematical problem defined by the Kohn–Sham (KS) equations.

Due to the electronic coupling and charge mobility in organic semiconducting material, DFT was considered befitting in calculating the charge transporting properties of the DPP–BTZ copolymer in terms of accuracy and computational efficiency for this large copolymer.

Recently, DFT simulation study employed the use of B3LYP functional because it combines Hartree–Fock exact exchange with DFT correlations in predicting HOMO (Highest Occupied Molecular Orbital) and LUMO (Lowest Unoccupied Molecular

Orbital) energies of organic semiconductors. This study took a step further in using a more accurate functional called CAM-B3LYP.

CAM-B3LYP is a hybrid functional which has specific features that address some limitations of local functionals such as B3LYP. It incorporates long-range correction (LC) which improves significantly the charge transporting character (the electronic excitation energies) for organic semiconductors. It also has a functional ability of handling non-local electron-electron interactions which makes it better in terms of accuracy for complex organic polymer such as DPP-BTZ copolymer, though it is computational expensive.

Basis sets are set of functions used to describe the wavefunctions of electrons in atoms and molecules. These functions form the foundation for approximating solutions to the Schrödinger equation in computational methods like Density Functional Theory (DFT) and Hartree-Fock (HF) calculations. 6-31G(d) was the basis set used for this study because it is a polarized basis set, thus it can account for the polarization of the electron clouds. Based on this feature, it offers a good description of charge distribution and polarization which is crucial in studying the charge transporting properties of organic semiconductors. 6-31G(d) is accurate, versatile and relatively computational inexpensive making it popularly used.

The DFT software packages used for this study used for Gaussian 09/ Gaussian 16 and Gauss view 5 as the Graphic User Interface. Though Molecular Dynamics software packages could have been used during the molecular stacking, a two-layered DPP-BTZ copolymeric stacks were developed using a vector mathematical approach using a π - π stacking distance of 3.5 Angstroms. These software packages

are running on the Linux mint Cinnamon where jobs were submitted or retrieved from the server using Linux terminal.

All the DPP–BTZ simulated structures were calculated at Geometry Optimization (Opt) + Frequency (Freq) Calculations concurrently. Whereas the “Opt” calculation computed their molecular geometry corresponding their minimum energy configuration, the “Freq” was computing their vibrational frequencies, assessing their thermodynamic properties and verifying the nature of stationary points whether minima or transition states.

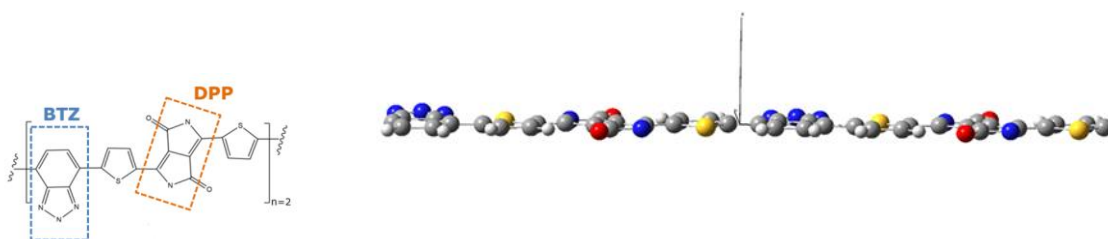
Also, the Self–Consistent Field (SCF) which is responsible for convergence, is an iterative process by solving the Schrödinger equation repeatedly, where each cycle refines the electron density using updated potential energies, which gradually converge towards a minima state that describes the electronic structure accurately. The default MaxCycle for many calculations is 64 iterations and 128 or 256 iterations for much complex systems but these DPP–BTZ conjugated copolymers employed at least 1,000 iterations per every single strand model and 5,000 iterations per every stacking configuration due to their nature and complexities.

Other robust convergence strategies like SCF= qc, xqc were also employed to enhance convergence process as well as reducing potential non–convergence errors in order to ensure accurate and reliable computational results.

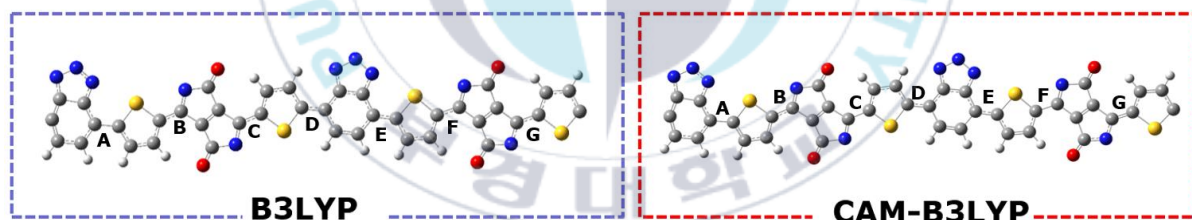
IV. Results & Discussion

The ultimate goal of this research was elucidated how side chain modifications influence the planarity of the DPP–BTZ copolymer backbone curvature. Understanding this correlation is crucial, since the planarity of the backbone curvature affects the electronic properties of conjugated polymers, which include charge transport efficiency and the overall performance of the device. By systematically modifying the side chains in terms of alkyl to fluoroalkyl ratio, we seek to establish an insightful correlation between side chains and backbone curvature, as a result providing comprehensive characterization designs of a high-performance organic semiconductors.

The planarity of DPP–BTZ conjugated polymers is extremely influenced by the torsional angles between adjacent DPP–BTZ monomeric units. These torsional angles dictate the degree of π -overlap along its backbone curvature, hence affecting the charge transporting properties along the DPP–BTZ dimeric backbone. The smaller the torsional angles, the more planar the backbone curvature of DPP–BTZ, and as a result enhancing the π -conjugation which facilitates efficient charge transport. On the contrary. The larger the torsional angles, the more distorted π -conjugation, which makes the backbone curvature less planar as a result of the twist hence hindering efficient charge transporting properties.



The choice of an appropriate density functional theory (DFT) functional was necessary for accurately simulating torsional angles along the DPP–BTZ backbone curvature at a Self–Consistent Field (SCF) method in order to ascertain the planarity of the DPP–BTZ conjugated polymer. Juxtaposing CAM–B3LYP and B3LYP DFT functionals, **CAM–B3LYP** is a range–separated hybrid functional, which incorporates long–range (LC) corrections that enhance its potential to handle long–range electron–electron interactions. This capability is important in accurately investigating and predicting the excited states, band gaps, and charge transporting properties of organic polymers such as DPP–BTZ conjugated polymer. On the contrary, B3LYP, a global hybrid functional, lacks the competence of long–range which makes it less accurate in predicting the long–range interactions even though it is relatively computational inexpensive.



	Bond	A	B	C	D	E	F	G
B3LYP	Torsional angle	178.64°	179.99°	179.96°	179.85°	-179.96°	-178.25°	175.65°
CAM-B3LYP	Torsional angle	177.25°	179.92°	179.97°	179.86°	179.92°	179.94°	179.99°

These torsional angles along the DPP–BTZ copolymer backbone were measured within the range of -180° to 180° . Both B3LYP and CAM–B3LYP functionals yielded nearly planar structures, with twist angle (torsional angle between the two DPP–BTZ monomers) **D**, determined as 0.15° for B3LYP and 0.14° for CAM–B3LYP. In

spite of the similarity in their nearly planar structures, CAM-B3LYP was chosen for further analysis due to its incorporated long-ranged (LC) corrections. These corrections enhance the ability of a DFT functional to accurately simulate long-range electron-electron interactions which are pivotal in elucidating the charge transporting properties of conjugated copolymers.

Among the numerous basis sets, the **6-31G(d) basis set** was befitting for this DPP-BTZ simulation because of it capturing the necessary electronic interactions effectively with manageable computational cost. The 6-31G(d) basis set is a split-valence double-zeta basis set, which means two basis functions for each valence orbital are used. The (d) in 6-31G(d) depicts the addition of polarization functions specifically, d-type functions on non-hydrogen atoms which accounts for the distortion of electron clouds during molecular interactions and bond formations leading to more accurate predictions of molecular geometries and electronic properties.

In order to systematically investigate into the influence of fluoroalkyl sidechains on DPP-BTZ backbone curvature in terms of planarity, a stepwise approach was adopted:

- a. **DPP-BTZ Backbone Curvature:** This approach is to analyze the integral torsional angles of DPP-BTZ dimer without side chains to serve as a benchmark in terms of planarity for the DPP-BTZ dimer.
- b. **DPP-BTZ dimer with Only Alkyl Side Chains:** Afterwards, alkyl side chains were fully introduced unto the DPP-BTZ backbone curvature in order to

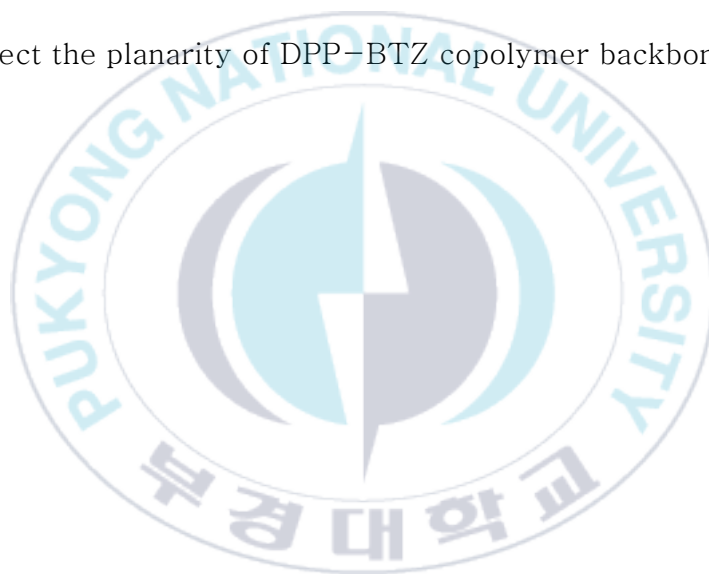
ascertain the effect of these alkyl side chains on the torsional angles of the DPP–BTZ backbone conformation.

- c. **DPP–BTZ dimer with Alkyl and Fluoroalkyl Side Chains:** Fluorine atoms were partially introduced in a halogenation reaction mechanism to form fluoroalkyl sidechains. This mechanism established a ratio between alkyl side chains and that of fluoroalkyl sidechains is 7:3, 5:5 and 3:7.
- d. **Comparing Root Mean Square (RMS) Values:** The root mean square of the values of degree of planarity needed to be calculated in order to ascertain the degree of planarity of the DPP–BTZ backbone curvature.
- e. **Stacking Configuration:** Finally, in order to investigate how π - π interactions affect the torsional angles of the DPP–BTZ backbone curvature with or without sidechains, a stacking configuration was developed using a mathematical approach with π - π distance of 3.5 angstroms.
- f. **DPP–BTZ Backbone Curvature Stacking Configuration:** This approach is to analyze how π - π interactions affect the integral torsional angles of DPP–BTZ dimer without side chains to serve as a benchmark in terms of planarity for the DPP–BTZ dimeric stack.
- g. **DPP–BTZ dimer with Only Alkyl Side Chains Stacking Configuration:** An alkyl side chains were fully introduced unto the DPP–BTZ backbone curvature in order to ascertain the effect of these alkyl side chains on the torsional angles in π - π interactions of the DPP–BTZ backbone conformation stack.
- h. **DPP–BTZ dimer with Alkyl and Fluoroalkyl Side Chains Stacking Configuration:** Fluorine atoms were partially introduced via a halogenation reaction mechanism to form fluoroalkyl sidechains in their π - π stacking

interactions. This mechanism established a ratio between alkyl side chains and that of fluoroalkyl sidechains is 7:3, 5:5 and 3:7 in their stacking configurations.

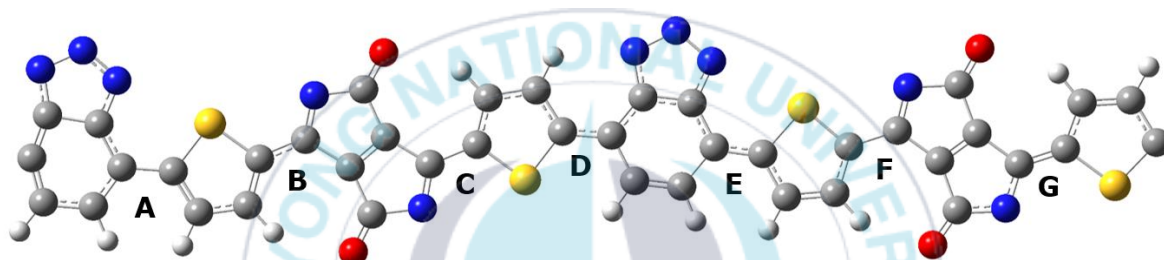
- i. **Comparing Root Mean Square (RMS) Values Stacking Configurations:** The root mean square of the values of degree of planarity needed to be calculated in order to ascertain the degree of planarity of the DPP–BTZ backbone curvature stacking configurations.

By employing these systematic mechanistic approaches in these DFT simulations, the results of torsional angles gave a comprehensive analysis as to how side chain modifications affect the planarity of DPP–BTZ copolymer backbone curvature.



A. DPP–BTZ Backbone Curvature

The DPP–BTZ backbone curvature serves as benchmark for the DPP–BTZ dimer with or without side chains. Experimental findings have established that the more planar and rigid the backbone of the conjugated polymer is, the more enhanced the efficiency of the charge transport. The torsional angles along the DPP–BTZ backbone were all nearly planar (close to $\pm 180^\circ$) with a calculated energy of -108.055 keV.



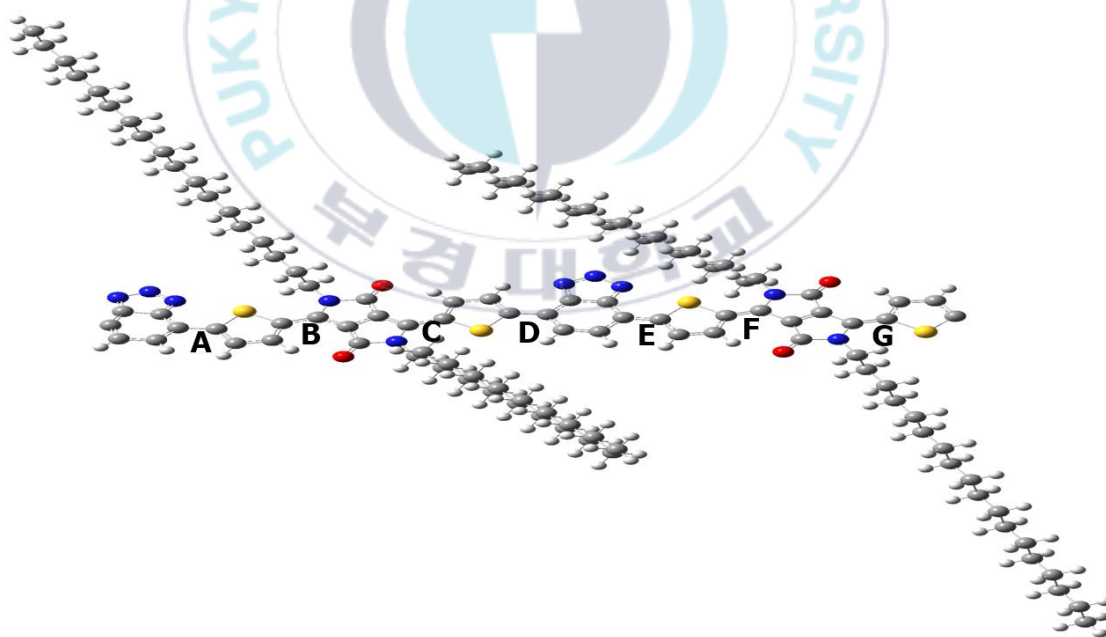
Bond	A	B	C	D	E	F	G
Torsional angle	177.25°	179.92°	179.97°	179.86°	179.92°	179.94°	179.99°

The torsional angles along the DPP–BTZ copolymer backbone were measured within the range of -180° to 180° . This reference results were instrumental in elucidating the impact of side chain modifications on the planarity of the backbone curvature of the DPP–BTZ conjugated copolymer by establishing a point of reference.

B. DPP–BTZ dimer with only Alkyl Side Chains (10:0)

– Alkyl to Fluoroalkyl sidechains ratio (10:0) approach

After simulating the DPP–BTZ without side chains, four (4) fully alkyl side chains ($C_{18}H_{37}$) were introduced unto the four (4) BTZ of the DPP–BTZ dimer. According to the experimental findings, this side chain architecture was found to facilitate good solubility and gave a high molecular weight conjugated polymers, which led to spontaneous chain crystallization. For this computational simulation, the “electron–donating” tendency of alkyl groups were investigated as to how their impact on the planarity of the DPP–BTZ backbone curvature on this side chain modifications architecture.



Bond	A	B	C	D	E	F	G
Torsional angle	-167.86°	178.85°	-179.22°	-179.70°	-179.03°	-178.43°	-178.36°

All the torsional angles were nearly planar (close to $\pm 180^\circ$) with a calculated energy of -185.100 keV. The torsional angles along the DPP–BTZ copolymer backbone were measured within the range of -180° to 180° .

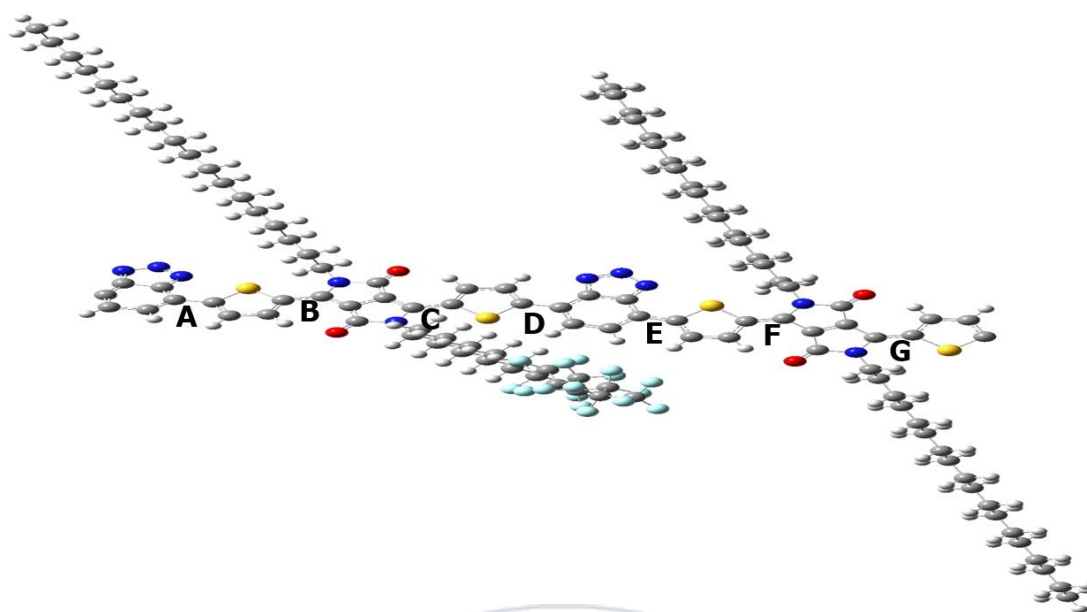


C. DPP–BTZ dimer with Alkyl and Fluoroalkyl Side Chains (7:3, 5:5, 3:7)

After simulating the DPP–BTZ with only alkyl side chains, seventeen (17) fluorine atoms were introduced systematically unto each alkyl side chains ($C_{18}H_{37}$) on the four (4) BTZ of the DPP–BTZ dimer via halogenation reaction mechanism. Experimentally, this halogenation reaction was done in an alkyl to fluoroalkyl sidechains ratios of 7:3, 5:5, and 3:7 respectively. Computationally, the “electron–withdrawing” tendency of fluorine atoms were investigated in that order to elucidate the influence of fluoroalkyl sidechains on the planarity of the DPP–BTZ backbone curvature.

– Alkyl to Fluoroalkyl sidechains ratio (7:3) approach

During this 7:3 sidechain engineering, the fluorine atoms were introduced on only one side chain with the rest of three sidechains remaining as alkyl sidechains. This strategic approach was to investigate the impact of the fluoroalkyl sidechain on the planarity of the DPP–BTZ backbone.



Bond	A	B	C	D	E	F	G
Torsional angle	-170.74°	-178.32°	-168.61°	-173.34°	-177.93°	-176.64°	-178.62°

Almost all the torsional angles were nearly planar (close to $\pm 180^\circ$) with a calculated energy of -230.99 keV. The torsional angles along the DPP-BTZ copolymer backbone were measured within the range of -180° to 180° .

– Alkyl to Fluoroalkyl sidechains ratio (5:5) approach

For the 5:5 sidechain engineering, the fluorine atoms were introduced in an equimolar ratio of alkyl to fluoroalkyl sidechains. This strategic approach allowed for a systematic investigation into the impact of this balanced equimolar (5:5) alkyl-halide substitution reaction on the planarity of the DPP-BTZ backbone.

There are three (3) conformational orientations for this 5:5 alkyl to fluoroalkyl sidechains which are **trans**–, **cis**– and **one-sided** conformers. These orientations were investigated in order to elucidate the exact conformation of the 5:5 alkyl to fluoroalkyl sidechains.

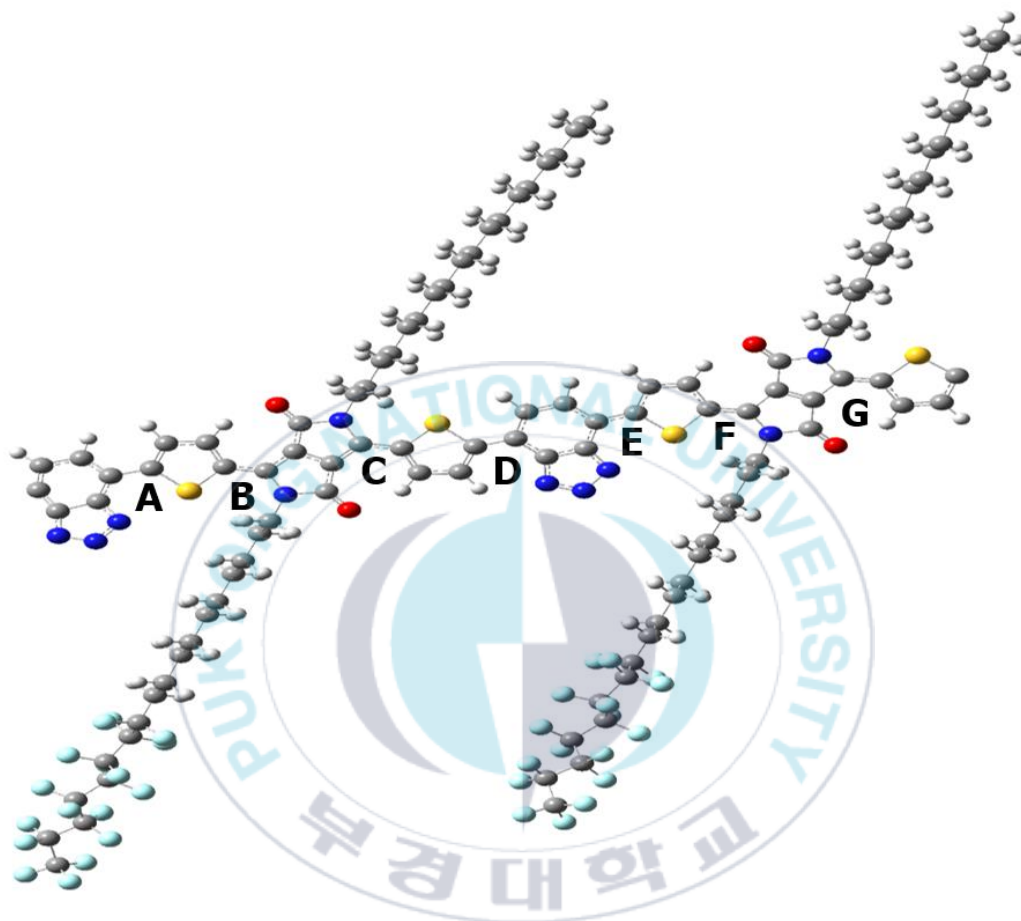
The **trans**– conformer was investigated first because of the most stable configuration tendencies for a 5:5 alkyl: fluoroalkyl substitution reaction.



Bond	A	B	C	D	E	F	G
Torsional angle	-164.43°	178.99°	176.18°	178.61°	-179.55°	-178.86°	-178.36°

Almost all the torsional angles were nearly planar (close to $\pm 180^\circ$) with a calculated energy of -276.89 keV. The torsional angles along the DPP–BTZ copolymer backbone were measured within the range of -180° to 180° .

The **cis** – conformer was investigated next because it is the second stable configuration for a 5:5 alkyl: fluoroalkyl substitution reaction which informed this kind of simulation modeling.

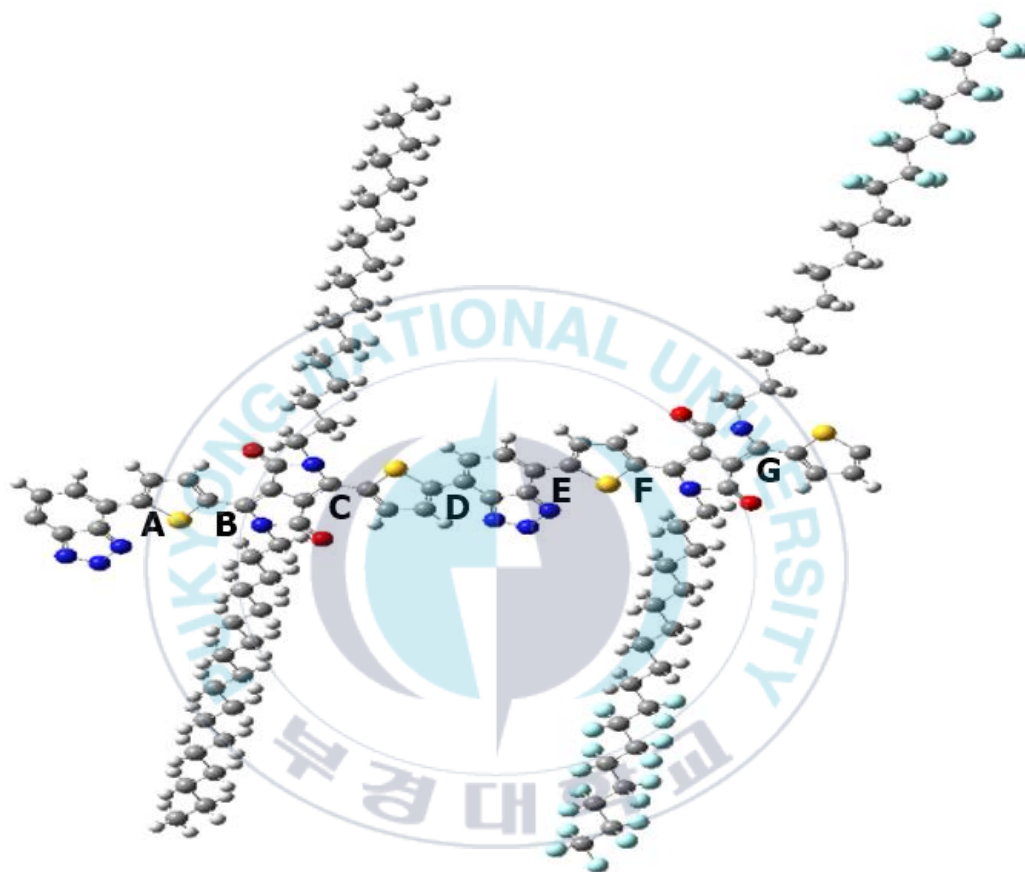


Bond	A	B	C	D	E	F	G
Torsional angle	-164.31°	178.76°	-176.69°	-177.83°	-179.17°	-179.03°	-179.32°

The torsional angles along the DPP–BTZ copolymer backbone were measured within the range of -180° to 180° . Almost all the torsional angles were nearly planar (close to $\pm 180^\circ$) with a calculated energy of -276.89 keV.

The **one sided** – conformer was investigated in order to elucidate all possible conformational orientations for a 5:5 alkyl: fluoroalkyl substitution reaction which

informed this kind of simulation modeling although the traditionally known orientations are the “cis-“ and “trans-“ conformations. This one sided-conformation is possible to occur in polymeric materials due to steric hindrances and most predominately electrophilic potency of sidechains.

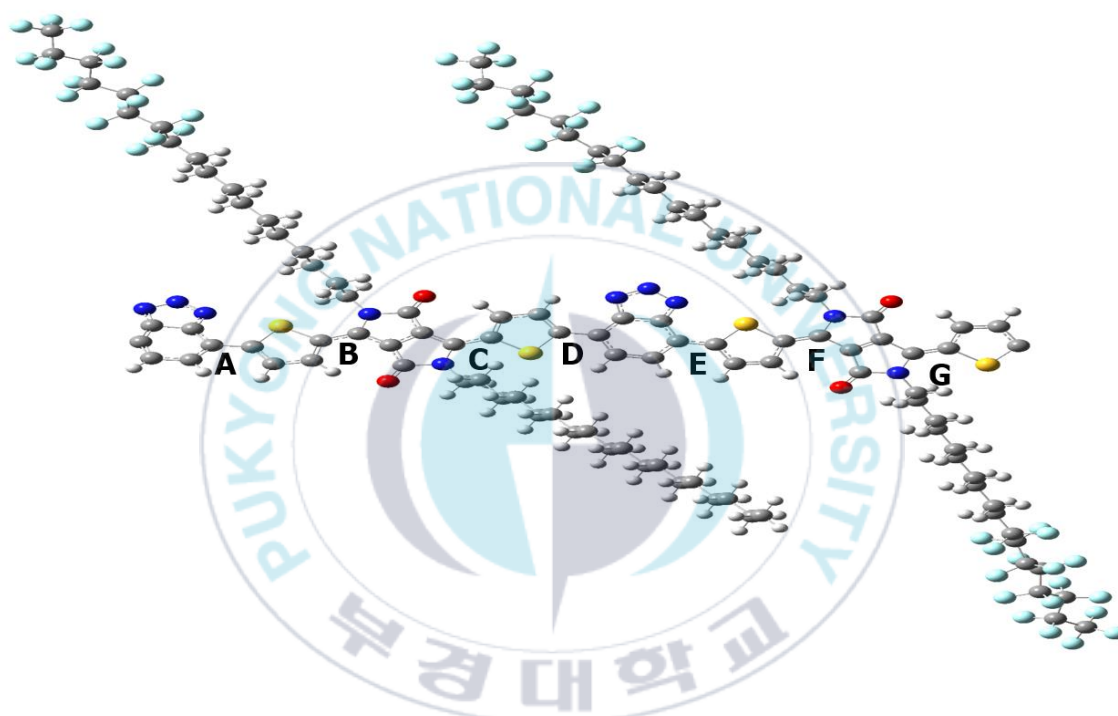


Bond	A	B	C	D	E	F	G
Torsional angle	-166.46°	-178.90°	-168.61°	-178.31°	-179.04°	-178.42°	-179.39°

The torsional angles along the DPP-BTZ copolymer backbone were measured within the range of -180° to 180° . Almost all the torsional angles were nearly planar (close to $\pm 180^\circ$) with a calculated energy of -276.89 keV.

– Alkyl to Fluoroalkyl sidechains ratio (3:7) approach

During this 3:7 sidechain engineering, the fluorine atoms were introduced onto three side chains remaining only one alkyl sidechains. This strategic approach was to investigate the impact of the many fluoroalkyl sidechains on the planarity of the DPP–BTZ backbone.



Bond	A	B	C	D	E	F	G
Torsional angle	-164.04°	-179.71°	-173.57°	-177.41°	-179.51°	-178.73°	-179.23°

The torsional angles along the DPP–BTZ copolymer backbone were measured within the range of -180° to 180° . Almost all the torsional angles were nearly planar (close to $\pm 180^\circ$) with a calculated energy of -322.793 keV.

D. Comparing Root Mean Square (RMS) Values

In order to ascertain the degree of planarity of the DPP–BTZ backbone curvature, the root mean square of the values of degree of planarity needed to be calculated. These calculations were done after subtracting the measured torsional angles from -180 or 180 depending on the sign of the measured torsional angles and then using the Root Mean Square equation to elucidate a comprehensive and insightful average of these positive and negative datasets. The equation is as below:

$$RMS = \sqrt{\frac{1}{n} \sum_i x_i^2}$$

RMS = root mean square

n = number of measurements

x_i = each value

Bond	A	B	C	D	E	F	G	RMS
Backbone Curvature	2.75°	0.08°	0.03°	0.14°	0.08°	0.06°	0.01°	1.042°
10:0	-12.14°	1.15°	-0.78°	-0.30°	-0.97°	-1.57°	-1.64°	4.713°
7:3	-9.26°	-1.68°	-11.39°	-6.66°	-2.07°	-3.36°	-1.38°	6.326°
5:5 (Cis)	-15.69°	1.24°	-3.31°	-2.17°	-0.83°	-0.97°	-0.68°	6.158°
5:5 (Trans)	-15.57°	1.01°	3.82°	1.39°	-0.45°	-1.14°	-1.64°	6.143°
5:5 (One-sided)	-13.54°	-1.10°	-11.39°	-1.69°	-0.96°	-1.58°	-0.61°	6.771°
3:7	-15.96°	-0.29°	-6.43°	-2.59°	-0.49°	-1.27°	-0.77°	6.604°

RMS = Root Mean Square (RMS) values along the DPP–BTZ Backbone curvature with/without alkyl– and fluoroalkyl– side chains.

All the possible conformations of the 5:5 alkyl-to-fluoroalkyl sidechain ratios were investigated in order to interpret an experimental trend that was observed as 10:0 ratio had the highest charge mobility, followed by 7:3 ratio and then 3:7 with 5:5 being the lowest in terms of charge mobility. The question as to how a 5:5 alkyl-to-fluoroalkyl sidechain ratio became the least charge mobility informed our investigation into the potential conformation that would have occurred during the 5:5 halogenation reaction.

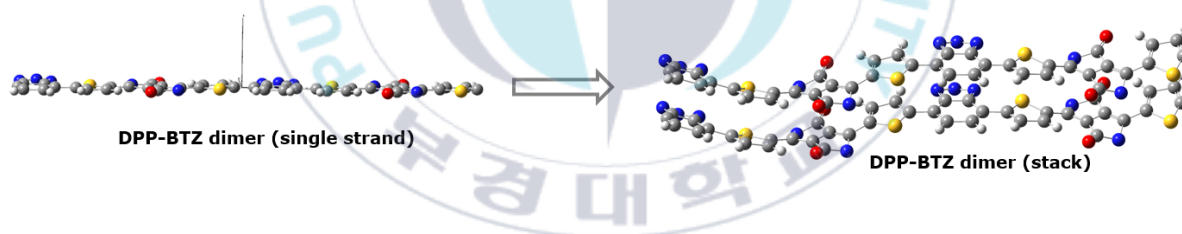
This RMS gave auxiliary insight of the average degree of planarity of the DPP-BTZ backbone even though individual torsional angles exhibited higher levels of planarity. From this result of varying alkyl-to-fluoroalkyl sidechain ratios, the 10:0 ratio demonstrated lower non-planarity which makes the highest planarity, followed by 7:3 ratio as higher planarity and then 3:7 ratio as moderate planarity while 5:5 (one sided) the lowest planar backbone conformation after these sidechain modifications.

This DFT simulation study validates the experimental findings and interpreting the spatial arrangement of the 5:5 alkyl-to-fluoroalkyl sidechain ratio which made to attain the least charge mobility. After these side chain engineering, a π - π stacking was mathematically developed for the DPP-BTZ backbone curvature and the various DPP-BTZ side chain ratios.

E. Stacking Configuration

The stacking approach was employed to investigate the impact of π - π interactions on the planarity of the DPP-BTZ dimer in a stacking configuration. This approach is crucial, as many polymers including DPP-BTZ conjugated copolymers, naturally adopt stacking conformations. The impact of the π - π interactions was determined using the DPP-BTZ without sidechains (backbone). By systematically analyzing these π - π interactions, the influence of the fluoroalkyl- sidechain(s) were investigated by elucidating the torsional and twist angles of the DPP-BTZ backbone curvature with sidechain modifications architecture.

The mathematical procedure for developing these DPP-BTZ stacking conformations are as follows:



- i. Locate three (3) non-collinear atoms.
- ii. Use these 3 atoms to find the two vectors that form a plane
- iii. Find the normal vector, \vec{k} .
- iv. Find the equation of the plane, $\mathbf{ax} + \mathbf{by} + \mathbf{cz} + \mathbf{d} = \mathbf{0}$, where $d =$ the dot product of the normal vector to one of the chosen atoms.
- v. Find the perpendicular plane, \vec{k} .

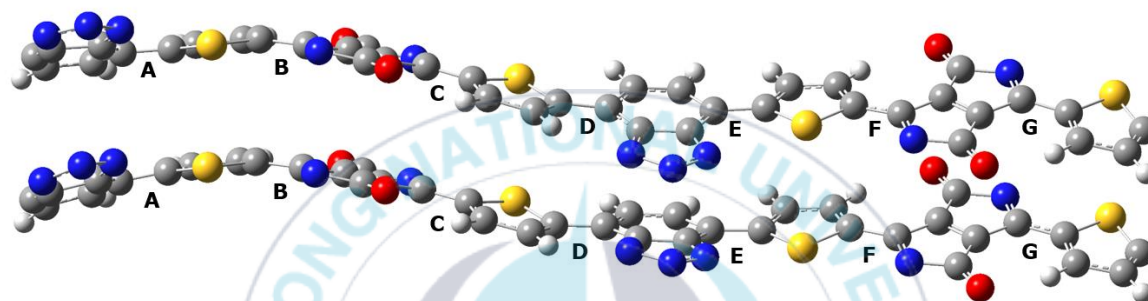
$$\hat{\mathbf{k}} = \frac{1}{\sqrt{a^2+b^2+c^2}} (a, b, c)$$

- vi. Using the $\hat{\mathbf{k}}$ to develop the XYZ coordinates for the second dimer to form a stack of distance 3.5 Angstroms.



F. DPP–BTZ Backbone Curvature Stacking Configuration

The DPP–BTZ backbone curvature serves as benchmark for the DPP–BTZ dimer with or without side chains. The efficiency of charge transport depends on rigidity and planarity of the conjugated polymer backbone. These π - π interactions enable delocalization of π -electrons between the adjacent molecules, creating charge carrier pathways (electrons and holes) for charge transporting properties.



Bond	A	B	C	D	E	F	G
Torsional angle (Both stacks)	-179.75°	-179.02°	-179.34°	179.79°	179.72°	-179.36°	-179.54°

All the torsional angles for both stacks were nearly planar (close to $\pm 180^\circ$).

The torsional angles along the DPP–BTZ copolymer backbone stack were measured within the range of -180° to 180° .

Comparing the torsional angles of the DPP–BTZ single strand to the torsional angles of the DPP–BTZ stack reveal a significant impact of the π - π interactions on the planarity of the DPP–BTZ copolymer backbone. These π - π interactions played a crucial role in modulating π -orbital overlapping in order to enhance planarity of the DPP–BTZ backbone.

G. DPP–BTZ dimer with only Alkyl Side Chains (10:0) Stacking Configuration

After simulating the DPP–BTZ stack without side chains, eight (8) fully alkyl side chains ($C_{18}H_{37}$) were introduced onto the eight (8) BTZ of the DPP–BTZ dimer stack. The “electron–donating” tendency of alkyl groups were investigated as to how their impact on the planarity of the DPP–BTZ stack backbone curvature for this side chain architecture.



Bond	A	B	C	D	E	F	G
Torsional angle (Both stacks)	178.39°	176.36°	178.15°	176.81°	177.83°	178.58°	179.47°

The torsional angles along the DPP–BTZ copolymer backbone stack were measured within the range of -180° to 180° . All the torsional angles for both stacks were nearly planar (close to $\pm 180^\circ$).

Comparing the torsional angles of this stacking approach to the torsional angles of the DPP–BTZ backbone curvature, it is evident that the nature of the sidechains

(longer alkyl- sidechains) played a pivotal role in enhancing the rigidity and overall planarity of the DPP-BTZ backbone curvature. This side-chain engineering ensured more planar and rigid DPP-BTZ backbone conformation which is crucial in charge transporting properties in conjugated polymers.

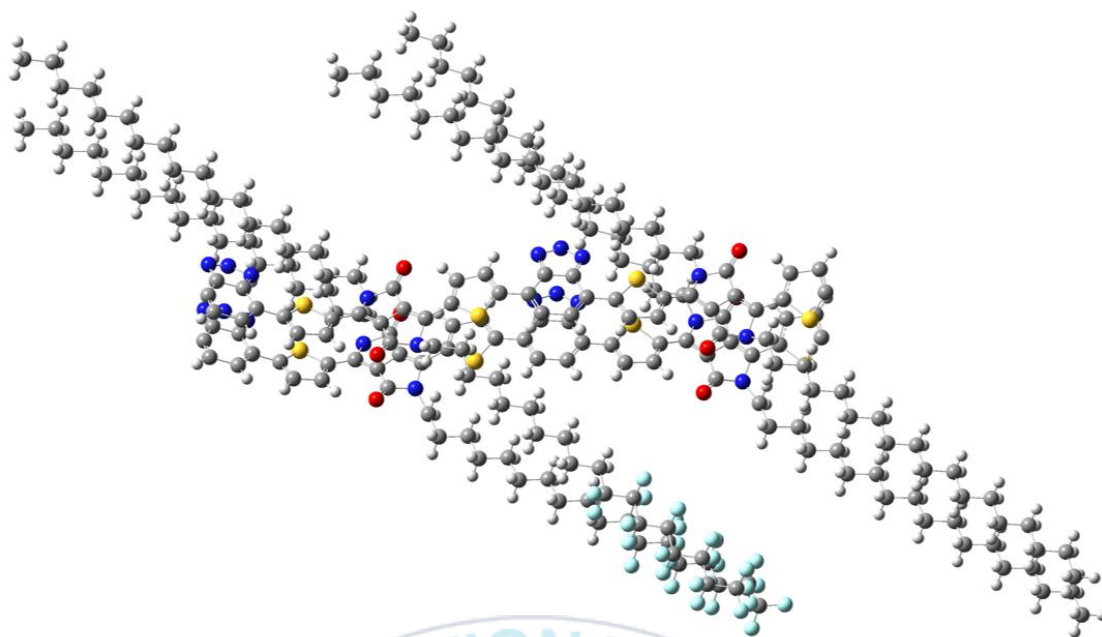


H. DPP–BTZ dimer with Alkyl and Fluoroalkyl Side Chains (7:3, 5:5, 3:7) Stacking Configuration

After simulating the DPP–BTZ stack with only alkyl side chains, seventeen (17) fluorine atoms were introduced systematically unto each alkyl side chains ($C_{18}H_{37}$) on the eight (8) BTZ of the DPP–BTZ dimer stack via halogenation reaction mechanism. Experimentally, this halogenation reaction was done in an alkyl to fluoroalkyl sidechains ratios of 7:3, 5:5, and 3:7 respectively. Computationally, the “electron–withdrawing” tendency of fluorine atoms were investigated in that order to elucidate the influence of fluoroalkyl sidechains on the planarity of the DPP–BTZ backbone curvature.

– Alkyl to Fluoroalkyl sidechains ratio (7:3) Stacking Approach

During this 7:3 sidechain engineering, the fluorine atoms were introduced on only one side chain with the rest of three set of sidechains remaining as alkyl sidechains. This strategic approach was to investigate the impact of the fluoroalkyl sidechains on the planarity of the DPP–BTZ backbone stack.



Bond	A	B	C	D	E	F	G
Torsional angle (Both stacks)	178.46°	176.30°	178.36°	176.13°	177.39°	177.79°	177.84°

All the torsional angles for both stacks were nearly planar (close to $\pm 180^\circ$). The torsional angles along the DPP–BTZ copolymer backbone stack were measured within the range of -180° to 180° .

The nature of the sidechains (longer alkyl– and fluoroalkyl– sidechains) played a crucial role in enhancing the rigidity and overall planarity of the DPP–BTZ backbone curvature. This side–chain engineering ensured more planar and rigid DPP–BTZ backbone conformation which is critical in charge transporting properties in conjugated polymers.

– Alkyl to Fluoroalkyl sidechains ratio (5:5) Stacking Approach

During this 5:5 sidechain engineering, the fluorine atoms introduced in an equimolar ratio of alkyl to fluoroalkyl sidechains. This strategic approach was to investigate the impact of a balanced fluoroalkyl sidechains on the planarity of the DPP–BTZ backbone stack.



Bond	A	B	C	D	E	F	G
Torsional angle	178.39°	176.36°	178.01°	176.17°	176.83°	177.21°	178.19°

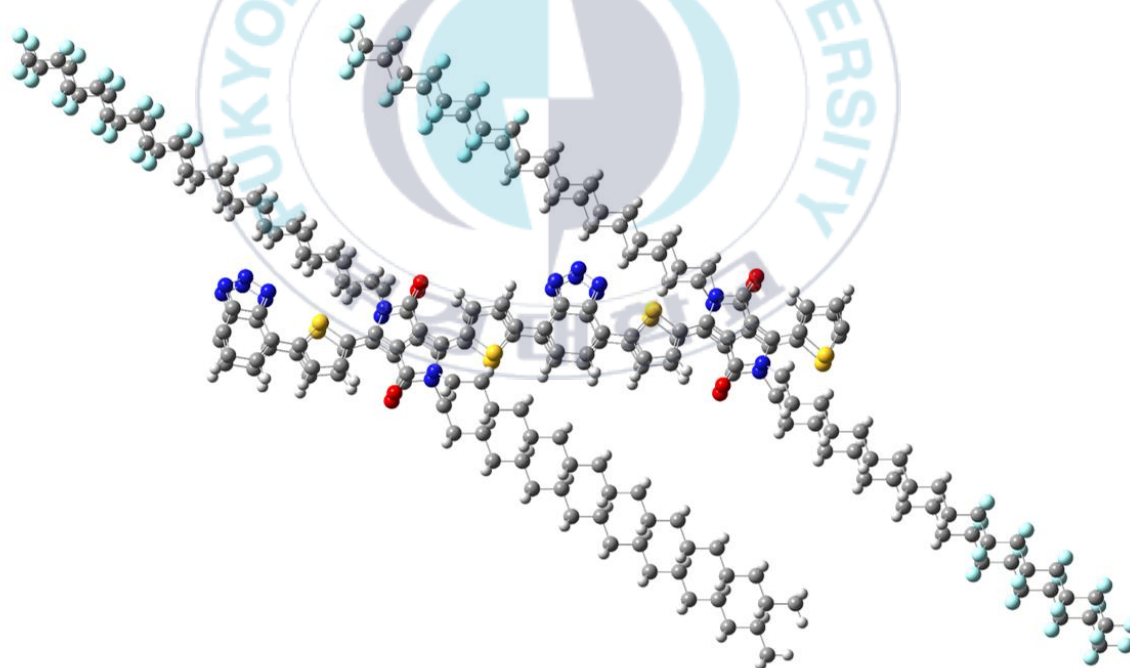
The torsional angles along the DPP–BTZ copolymer backbone stack were measured within the range of -180° to 180° . All the torsional angles for both stacks were nearly planar (close to $\pm 180^\circ$).

The nature of the sidechains (longer alkyl– and fluoroalkyl– sidechains) played a crucial role in enhancing the rigidity and overall planarity of the DPP–BTZ

backbone curvature. This side-chain engineering ensured more planar and rigid DPP-BTZ backbone conformation which is critical in charge transporting properties in conjugated polymers.

– Alkyl to Fluoroalkyl sidechains ratio (3:7) Stacking Approach

During this 3:7 sidechain engineering, the fluorine atoms were introduced on three set of side chains remaining only one set of sidechains as alkyl sidechains. This strategic approach was to investigate the impact of the fluoroalkyl sidechains on the planarity of the DPP-BTZ backbone stack.



Bond	A	B	C	D	E	F	G
Torsional angle (Both stacks)	178.39°	175.69°	178.15°	176.81°	177.09°	177.29°	178.28°

The torsional angles along the DPP–BTZ copolymer backbone stack were measured within the range of -180° to 180° . All the torsional angles for both stacks were nearly planar (close to $\pm 180^\circ$).

The nature of the sidechains (longer alkyl– and fluoroalkyl– sidechains) played a crucial role in enhancing the rigidity and overall planarity of the DPP–BTZ backbone curvature. This side–chain engineering ensured more planar and rigid DPP–BTZ backbone conformation which is critical in charge transporting properties in conjugated polymers.



I. Comparing Root Mean Square (RMS) Values of the Stacking Configurations

In order to ascertain the degree of planarity of the DPP–BTZ backbone curvature, the root mean square of the values of degree of planarity needed to be calculated. These calculations were done after subtracting the measured torsional angles from -180 or 180 depending on the sign of the measured torsional angles and then using the Root Mean Square equation to elucidate a comprehensive and insightful average of these positive and negative datasets. The equation is as below:

$$RMS = \sqrt{\frac{1}{n} \sum_i x_i^2}$$

RMS = root mean square
n = number of measurements
x_i = each value

Bond	A	B	C	D	E	F	G	RMS
Backbone Curvature	-0.25°	-0.98°	-0.66°	0.21°	0.28°	0.64°	0.46°	0.561°
10:0	1.61°	3.64°	1.85°	3.19°	2.17°	1.42°	0.53°	2.282°
7:3	1.54°	3.70°	1.64°	3.12°	2.61°	2.21°	2.16°	2.591°
5:5	1.61°	3.64°	1.99°	3.83°	3.17°	2.79°	1.81°	2.818°
3:7	1.61°	4.31°	1.85°	3.19°	2.91°	2.71°	1.72°	2.763°

RMS = Root Mean Square (RMS) values along the DPP–BTZ Backbone curvature with/without alkyl– and fluoroalkyl– side chains.

This RMS gave auxiliary insight of the average degree of planarity of the DPP–BTZ backbone even though individual torsional angles exhibited higher levels of planarity. From this result of varying alkyl–to–fluoroalkyl sidechain ratios for the stacking configurations, the 10:0 ratio demonstrated lower non–planarity which

makes the highest planarity, followed by 7:3 ratio as higher planarity and then 3:7 ratio as moderate planarity while 5:5 the lowest planar backbone conformation after these sidechain engineering.

This DFT simulation study validates the experimental findings and interpreting that was observed as 10:0 ratio had the highest charge mobility, followed by 7:3 ratio and then 3:7 with 5:5 being the lowest in terms of charge mobility.



V. Conclusion

The planarity of DPP–BTZ conjugated polymers play a crucial role in the efficiency of their charge transporting properties. The tendency of a DPP–BTZ copolymer to be planar, mostly depends on the side chain engineering and seldomly depends on the π - π interactions. Hence, in order to modify the efficiency of an organic semiconducting conjugated copolymer, side chain engineering must be an utmost priority other than the stacking conformations.

The measurement of torsional angles was used to ascertain the planarity of the various DPP–BTZ dimeric units with their root mean square values elaborating the degree of planarity for each systematic approach.

The tendencies of fluoroalkyl– sidechains to act as both electrophiles and nucleophiles, influenced the nature of the backbone curvature although fluorine atoms are electrophiles. The nature of the side chains also played a pivotal role in enhancing the planarity of the DPP–BTZ conjugated copolymer especially during the stacking configurations.

This DFT simulation study has provided a mechanistic insight into the experimental findings observed during the experimental study and thus there is a synergy between the computational study and that of the experiment hence validating and interpreting the spatial arrangement of the DPP–BTZ conjugated copolymer in their dimeric units.

References

- [1] Shirakawa, H., Louis, E. J., MacDiarmid, A. G., Chiang, C. K., & Heeger, A. J. (1977). Synthesis of electrically conducting organic polymers: Halogen derivatives of polyacetylene, $(\text{CH})_x$. *Journal of the Chemical Society, Chemical Communications*, (16), 578–580.
- [2] Chen, C. H., Klubek, K. P., Van Slyke, S. A., & Tang, C. W. (1998). Fluorescent Dopants in Organic Electroluminescent Devices. In *Proceedings of the SPIE Conference on Display Technologies II* (Vol. 3421, pp. 78–82). SPIE.
- [3] Klauk, H., Gundlach, D. J., Nichols, J. A., & Jackson, T. N. (1999). Pentacene-based organic thin-film transistors. *IEEE Transactions on Electron Devices*, 46(7), 1258–1263.
- [4] Ong, B. S., Wu, Y., Liu, P., & Gardner, S. (2004). High-performance semiconducting polythiophenes for organic thin-film transistors. *Journal of the American Chemical Society*, 126(10), 3378–3379.
- [5] McCulloch, I., Heeney, M., Bailey, C., Genevicius, K., MacDonald, I., Shkunov, M., Sparrowe, D., Tierney, S., Wagner, R., Zhang, W., Chabinyc, M. L. (2006).

Liquid-crystalline semiconducting polymers with high charge-carrier mobility. *Nature Materials*, 5(4), 328–333.

[6] Marina, S., Gutierrez-Fernandez, E., Gutierrez, J., Gobbi, M., Ramos, N., Solano, E., Rech, J., You, W., Hueso, L., Tercjak, A., Ade, H., & Martin, J. (2022). Semi-paracrystallinity in semi-conducting polymers. *Materials Horizons*, 9(4), 1196–1206.

[7] Matyba, P., Maturova, K., Kemerink, M., Robinson, N. D., & Edman, L. (2009). The dynamic organic p-n junction. *Nature Materials*, 8, 672–676.

[8] Reynolds, J. R., Thompson, B. C., & Skotheim, T. A. (Eds.). (2019). *Conjugated Polymers: Perspective, Theory, and New Materials*. CRC Press.

[9] Havinga, E. E., ten Hoeve, W., & Wynberg, H. (1992). A new class of small band gap organic polymer conductors. *Polymer Bulletin*, 29(1), 119–126.

[10] Nielsen, C. B., Turbiez, M., & McCulloch, I. (2012). Recent advances in the development of semiconducting DPP-containing polymers for transistor applications. *Advanced Materials*, 24(37), 503–515.

[11] Gruber, M., Jung, S.-H., Schott, S., Venkateshvaran, D., Kronemeijer, A. J., Andreasen, J. W., Sirringhaus, H. (2015). Enabling high-mobility, ambipolar charge-transport in a DPP-benzotriazole copolymer by side-chain engineering. *Chemical Science*, 6, 6949-6960.

[12] Marina, S., Gutierrez-Fernandez, E., Gutierrez, J., Gobbi, M., Ramos, N., Solano, E., Rech, J., You, W., Hueso, L., Tercjak, A., Ade, H., & Martin, J. (2022). Semi-paracrystallinity in semi-conducting polymers. *Materials Horizons*, 9(4), 1196-1206.

[13] Raychev, D., Mendez Lopez, R. D., Kiriy, A., Seifert, G., Sommer, J.-U., & Guskova, O. (2019). Copolymers of Diketopyrrolopyrrole and Benzothiadiazole: Design and Function from Simulations with Experimental Support. *Macromolecules*, 52(3), 904-914.

The Influence of Fluoroalkyl Side-Chain Ratio on Charge Transporting Properties in DPP-BTZ Copolymer Film: A DFT Simulation Study with Experimental Support

Bright Aryeh Afriyie

Dept. of Smart Green Technology Engineering, The Graduate school,

Pukyong National University

Abstract

In the pursuit of advancing the frontiers of organic field-effect transistors, Diketopyrrolopyrrole (DPP) -based donor-acceptor (D-A) type copolymers are earning keen research interests due to their high field-effect mobility coupled with the ambipolar characteristics within which both p-type and n-type charge can occur along a backbone curvature. In this Density Functional Theory (DFT) simulation study, the focus was on determining the planarity of the backbone curvature of the Diketopyrrolopyrrole-Benzotriazole (DPP-BTZ) copolymer chain in giving an in depth understanding the charge transporting properties that occurred experimentally. Also, the side-chain engineering was considered in ratios of alkyl: fluoroalkyl side chains of 10:0, 7:3, 5:5, and 7:3 where the influence of the fluorine has on the planarity of the DPP-BTZ backbone curvature using torsional angles and energetics. Stacking of the DPP-BTZ copolymer was also crucial in determining the planarity of the copolymer at a π - π stacking distance of 3.5 Angstroms. In conclusion, this study with experimental support elucidates that the planarity of the backbone curvature under the influence of side-chain engineering, is essential for efficient charge transport in order to design a high-performance D-A type semiconducting copolymer.